NUSC Technical Document 8783
5 October 1990

Low Frequency Noise From Breaking Waves

An Invited Paper Presented at the Conference on Natural Physical Sources of Underwater Sound, University of Cambridge, July 1990

William M. Carey
Technology Coordination Office

James W. Fitzgerald
Kildare Corporation

David G. Browning
Environmental and Tactical
Support Systems Department

AD-A227 969

DTIC
ELECTE
OCT 30 1990
S E D

Naval Underwater Systems Center
Newport, Rhode Island • New London, Connecticut

Approved for public release; distribution is unlimited.

PREFACE

This report contains an invited paper given at the Conference on Natural Physical Sources of Underwater Sound at the University of Cambridge, July 1990. It was written under the partial sponsorship of Dr. M. Orr, Office of Naval Research (Code 1125OA), and Dr. K. Lima, Naval Underwater Systems Center (Code 10).

The results presented in this paper are the cummulation of work begun in 1980 and supplement the results presented at the Nato Advanced Workshop on the Natural Mechanisms of Surface Generated Noise in the Ocean held in Lerici, Italy, in 1987, and published in Sea Surface Sound. The paper, "Low Frequency Ocean Ambient Noise: Measurement and Theory," is included here as an appendix.

REVIEWED AND APPROVED: 5 October 1990

D. M. VICCIONE
ASSOCIATE TECHNICAL DIRECTOR FOR
RESEARCH AND TECHNOLOGY

REPORT DOCUMENTATION PAGE

Form Approved
OMB No. 0704-0188

Public reporting burden for this collection of information is estimated to average 1 hour per response, including the time for reviewing instructions, searching existing data sources, gathering and maintaining the data needed, and completing and reviewing the collection of information. Send comments regarding this burden estimate or any other aspect of this collection of information, including suggestions for reducing this burden, to Washington Headquarters Services, Directorate for Information Operations and Reports, 1215 Jefferson Davis Highway, Suite 1204, Arlington, VA 22202-4302, and to the Office of Management and Budget, Paperwork Reduction Project (0704-0188), Washington, DC 20503

1. AGENCY USE ONLY *(Leave blank)*

2. REPORT DATE
5 October 1990

3. REPORT TYPE AND DATES COVERED
Presentation

4. TITLE AND SUBTITLE
Low Frequency Noise From Breaking Waves

5. FUNDING NUMBERS
A60460

6. AUTHOR(S)
William M. Carey, James W. Fitzgerald (Kildare Corp.), David G. Browning

7. PERFORMING ORGANIZATION NAME(S) AND ADDRESS(ES)
Naval Underwater Systems Center
New London Laboratory
New London, CT 06320

8. PERFORMING ORGANIZATION REPORT NUMBER
TD 8783

9. SPONSORING/MONITORING AGENCY NAME(S) AND ADDRESS(ES)

10. SPONSORING/MONITORING AGENCY REPORT NUMBER

11. SUPPLEMENTARY NOTES

12a. DISTRIBUTION/AVAILABILITY STATEMENT
Approved for public release; distribution is unlimited.

12b. DISTRIBUTION CODE

13. ABSTRACT *(Maximum 200 words)*

This document contains an invited paper given at the Conference on Natural Physical Sources of Underwater Sound at the University of Cambridge, July 1990.

Recent experiments confirm the production of sound by breaking waves at lower frequencies (30 to 500 Hz). Individual breakers produce impact noise as well as a random collection of individual spectral events. Measured ocean ambient noise spectrum levels increase at less than 1 dB per octave toward a broad maximum, which has a weak wind speed dependence between 300-500 Hz. Noise intensities (< 500 Hz) are a function of wind speed (U) to the 2n power with $1.3 < n < 2.5$ and a value of n=1.5 at 200 Hz. The production of noise in this region has a dipole characteristic. Breaking waves produce an impact, bubble plume, and bubble cloud. The dynamic evolution of these plumes and clouds provides a mechanism for sound production. Since the initial plume and cloud have appreciable void fractions, compressible resonant behavior of these structures as a whole or as multiply connected regions can be represented as compact acoustic monopoles and dipoles.

14. SUBJECT TERMS

15. NUMBER OF PAGES

16. PRICE CODE

17. SECURITY CLASSIFICATION OF REPORT	18. SECURITY CLASSIFICATION OF THIS PAGE	19. SECURITY CLASSIFICATION OF ABSTRACT	20. LIMITATION OF ABSTRACT
Unclassified	Unclassified	Unclassified	SAR

13. ABSTRACT (Cont'd.)

The pressure release surface would result in an effective dipole characteristic. Sufficient energy exists in the initial breaking vorticity and turbulence to explain measured source levels. Since a good radiator of sound is also a scatterer of sound, these plumes and clouds will also scatter sound.

ion For
GRA&I ☒
TAB ☐
ounced ☐
Justification
By
Distribution/
Availability Codes
Dist | Avail and/or Special
A-1

LOW FREQUENCY NOISE FROM BREAKING WAVES

William M. Carey and James W. Fitzgerald*
Naval Underwater Systems Center
New London, Connecticut 06320
USA

ABSTRACT. Recent experiments confirm the production of sound by breaking waves at lower frequencies (30 to 500 Hz). Individual breakers produce impact noise as well as a random collection of individual spectral events. Measured ocean ambient noise spectrum levels increase at less than 1 dB per octave toward a broad maximum, which has a weak wind speed dependence between 300 to 500 Hz. Noise intensities (< 500 Hz) are a function of wind speed (U) to the 2n power with $1.3 < n < 2.5$ and a value of n=1.5 at 200 Hz. The production of noise in this region has a dipole characteristic. Breaking waves produce an impact, bubble plume, and bubble cloud. The dynamic evolution of these plumes and clouds provides a mechanism for sound production. Since the initial plume and cloud have appreciable void fractions, compressible resonant behavior of these structures as a whole or as multiply connected regions can be represented as compact acoustic monopoles and dipoles. The pressure release surface would result in an effective dipole characteristic. Sufficient energy exists in the initial breaking vorticity and turbulence to explain measured source levels. Since a good radiator of sound is also a scatterer of sound, these plumes and clouds will also scatter sound.

1. INTRODUCTION

In his review of Ambient Noise in the Sea, Urick (1984) commented on the prolific nature of literature concerning theories of sound generation at the sea surface and the measurements of the temporal and spatial spectral characteristics. The idealized spectra suggested by Urick was in close agreement with the schematic proposal by Wenz (1962). The spectral characteristics for frequencies greater than 500 Hz are consistent with the observations of Knudsen (1948) and Wenz's "rule of fives" that the noise level can be described by

$$NL(f,U) = 25 - 5LOG(f) + 5LOG(U/5) \quad [\text{dB re } 20\ \mu N/m^2] \ ,$$

* Kildare Corporation, 95 Trumbull Street, New London, CT 06320 USA.

where f is frequency (kHz) and U is wind speed (knots). However, as Wenz observed in the 10- to 500-Hz band, the measured noise levels were often variable and dominated by shipping noise. The shape of the spectrum was also found to vary from a positive slope to a steep negative slope.

Kerman (1984) showed that "the amalgamated observations of the ambient noise reveal a similarity structure, both in the acoustical spectrum and wind dependency." For frequencies greater than the local maximum in the 300- to 500-Hz range, Kerman found that the normalized measured spectral characteristic was proportional to f^{-2}(6 dB/octave). Furthermore, he showed that the noise intensity was proportional to the cube of the friction velocity (u_*^3) prior to a critical friction velocity (u_{*c}) which is determined by the minimum phase velocity of the gravity-capillary waves. Wave breaking was associated with this critical condition, and for $u_* > u_{*c}$ the noise intensity was found to increase with $u_*^{1.5}$. These observations were found to be consistent with a large number of experimental observations cited by Kerman. He speculated that the two observed regions of ambient noise wind speed dependency indicated the presence of two sound source generation mechanisms or one mechanism that changes sensitivity. Nevertheless, since breaking waves are known to produce bubbles, spray, splash, and turbulence, combinations of these mechanisms may explain the production of sound at frequencies >500 Hz. Kerman also observed a variability in the region <500 Hz.

At frequencies <500 Hz, it has been difficult to acquire ambient noise data that are attributable solely to local effects. The reason for this is the dominance of shipping noise in the Northern Hemisphere, the problems of self-noise, the size required for directional measurement systems, and the relatively low long range propagation loss.

Reviews of low- to mid-frequency (20 to 1000 Hz) ambient noise measurements (Carey (1985,1988)) not dominated by shipping at frequencies <500 Hz showed the presence of locally wind-generated noise. Wittenborn (1976) showed a wind speed dependence with a linear velocity dependence prior to u~6 m/s and a quadratic dependence at greater wind speeds. His results were not based on actual local measurements of environmental variables such as wind speed. Measurements performed with vertical arrays in the sparsely shipped Southern Hemisphere's Fiji Basin (Bannister (1981), Burgess and Kewley (1983), Browning (1986)) were also found to have low frequency wind noise with two distinct wind speed dependencies. When compared to other shallow and deep water noise measurements, these results led to the conclusion that at the lower frequencies sound was generated near the sea surface with one wind speed dependent mechanism prior to wave breaking and another after wave breaking (Carey (1985,1988)).

Two interesting experiments have recently been performed featuring visual as well as acoustic identification of wave breaking events. Hollett (1988) performed an experiment in the Mediterranean Sea with a vertical array of hydrophones (3 nested apertures (32 phones each) with center frequencies at 375, 750, and 1500 Hz) and simultaneous video recording of the sea surface area intersected by the endfire beam of the array. Figure 1 shows the spectral events which result from a

large breaker. The spectra shown have not been corrected for the prewhitening of the data; i.e., the lower frequency spectral content is more pronounced than shown. The breaking event occurs between 3 to 7 seconds and is seen to be a random collection of spectral peaks most pronounced in the low frequency (<300 Hz) range.

Farmer (1989) performed an experiment in 200 m of water with a hydrophone 14 m below the surface and was able to identify the occurrence of wave breaking by examining the video obtained from a subsurface camera. The simultaneously recorded acoustic data were examined and found to show that the breaking waves radiate sound to frequencies as low as 50 Hz.

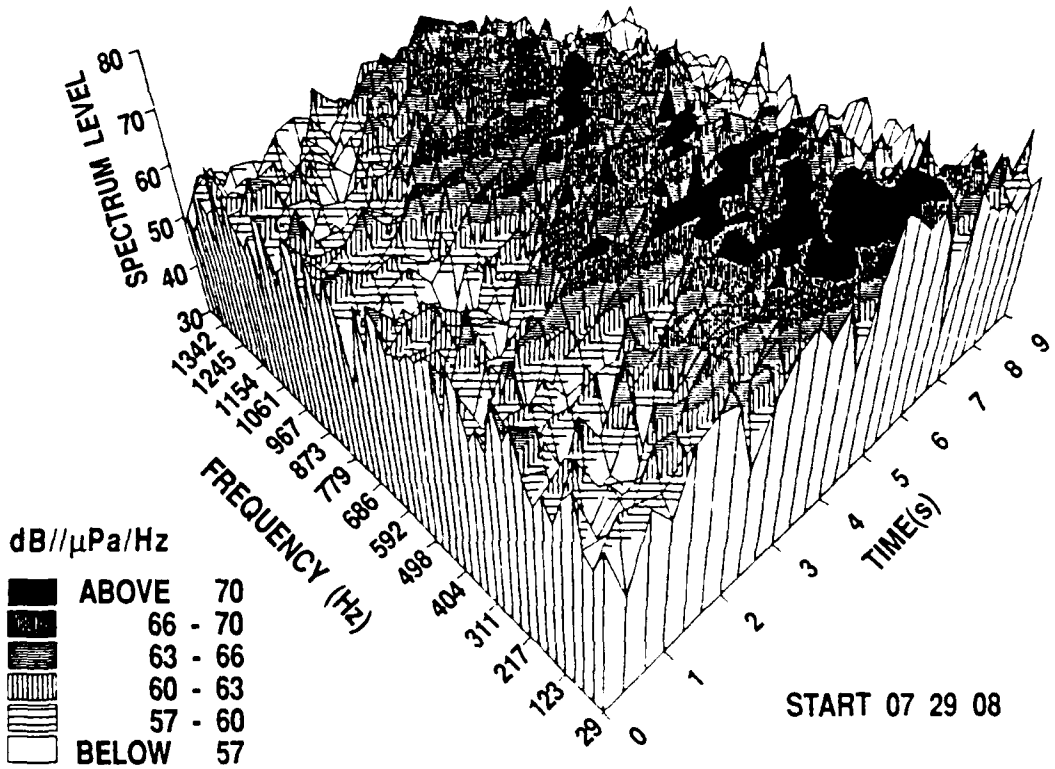

Figure 1. Spectra of a wave breaking as measured by Hollett (1988) are shown as a function of time. The lower frequency spectral estimates have not been corrected for pre-emphasis. This collection of acoustic spectra shows the wave breaking event to be a random collection of spectral peaks.

The Hollett and Farmer results clearly show that breaking waves are a source of low frequency sound and that at frequencies < 500 Hz the ambient noise spectrum in the absence of shipping is wind speed dependent. These results are important with respect to measurements performed with vertical and horizontal arrays where the directional noise properties, in the absence of shipping, are due to the interaction of wind-generated noise and the basin boundaries.

Since breaking waves produce sound at frequencies < 500 Hz, a question concerning the generating mechanisms naturally arises. This paper shall examine the role of spray, impact, and the collective oscillations of bubble plumes and clouds proposed by this author and Prosperetti (1985). First, the properties of low frequency ambient noise in terms of the wind speed dependence and spectral characteristic will be presented. This section will feature recent experimental work since the Lerici meeting (Carey (1988)). Second, the properties of mixtures will be discussed and theoretical expressions for spherical and cylindrical bubble clouds presented. Calculations will be presented for the noise production in a hypothetical wave breaking event based on an evolution model due to Monahan that demonstrates that bubble plume and cloud oscillation are candidate mechanisms for the production of noise.

2. A REVIEW OF RECENT LOW FREQUENCY NOISE MEASUREMENTS

Since a voluminous amount of ambient noise literature exists (Urick (1984), Kerman (1984), (1988)), the purpose of this review is to simply concentrate on ambient noise characteristics <500 Hz. This characterization will be based on the determination of two parameters, the spectral slope m(f) and the wind speed dependency n(f) defined by

$$\Delta NL(f,f_o,U,U_o) = 20n(f)LOG(U/U_o) + 10m(f)\cdot LOG(f/f_o),$$

where ΔNL is the difference in measured noise level at frequencies f and f_o and wind speeds U and U_o. These parameters are usually estimated by the use of regression analysis and, in some instances, by a visual least-squares estimation. We have previously stated that the measurement of low frequency wind-dependent noise is difficult due to the presence of shipping noise, self-noise, and sound propagation conditions. For this reason, we have been selective with respect to those measurements included in this summary.

2.1 The Low Frequency Spectral Slope

In a previous paper (Carey (1988)), the experimental results from Wittenborn (1976) were presented as an example of deep ocean wind-generated ambient noise. This experiment consisted of a vertical string of omnidirectional hydrophones, one of which was positioned below the sound channel's critical depth to minimize the hydrophone's reception of distant generated noise. Additional results from this experiment may be found in a recent article by Shooter, De Mary, and Wittenborn (1990). The hydrophone data were remotely recorded on a time-indexed magnetic tape. Wind speed estimates were based on interpolating weather reports of ships transiting the area. Stationary periods were selected by examining the continuous recording of the 300- to 500-Hz band of the deep hydrophone. However, the lack of concurrent wind speed and air-sea temperature difference is a major shortcoming of this experiment. Nevertheless, the results clearly show wind-dependent

noise characteristics between 20 and 500 Hz. The 15-knot curve shown in Fig. 2 has spectral slopes of m=0,1,1/3. The corresponding wind speed factor (n) determined by the difference in noise levels at 12 and 15 knots and a frequency of 100 Hz was n=1.65.

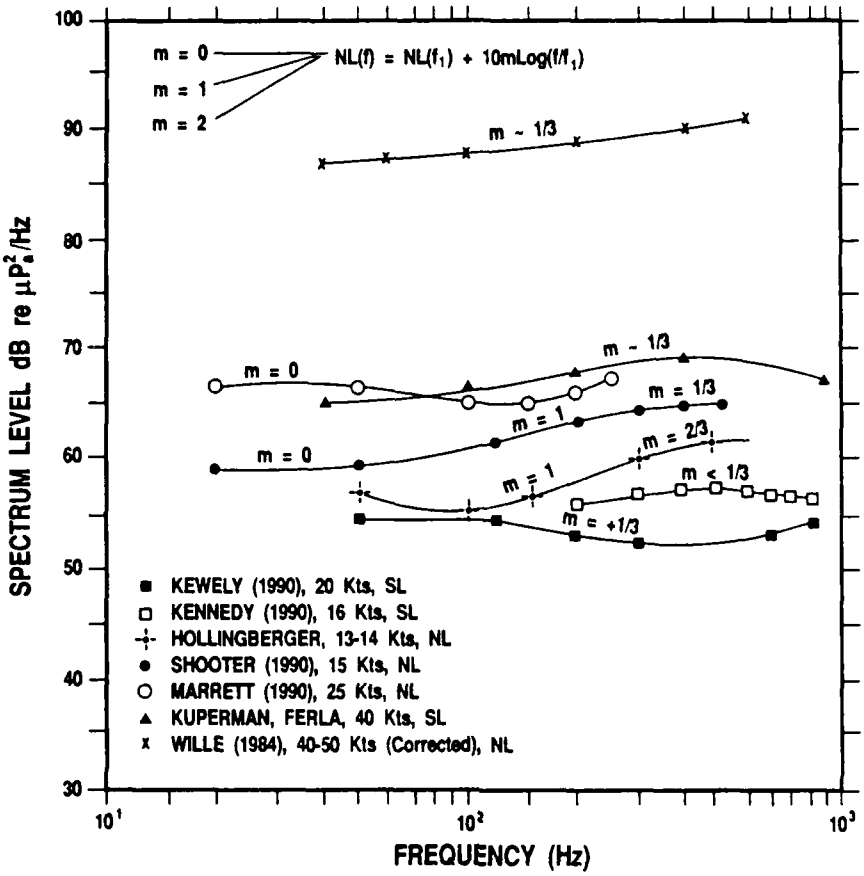

Figure 2. Source spectrum level (SL) and noise spectrum level (NL) are shown on this plot of spectrum level vs frequency for wind speeds >13 knots for several diverse oceanographic areas.

Several investigators have used vertical arrays to measure the locally generated noise in deep water. Most notable are the works of Burgess and Kewley (1983) in the South Fiji Basin and Australian waters and Kennedy (1990) in the Tongue of the Ocean in the Bahamas. In addition to the use of steerable arrays, these experiments were conducted in areas to minimize shipping noise and had concurrent measurement of wind speed.

The Burgess and Kewley (1983) experiment used a 180-m steerable array at a depth of 300 m in deep water to avoid mixed layer ducting effects. Both upward and downward looking beams were used to determine the sea surface source level (SL), dB re 1 $\mu Pa^2/(sr \cdot Hz)$. Since their original publication, these authors have re-examined their linear regression analysis of the wind speed dependency and have concluded that two wind speed dependent regions exist, i.e., one prior to and one after the onset of wave breaking with n~1.5 (Kewley et al. (1990)).

Their frequency-dependent source level estimate is shown in Fig. 2. In examining Fig. 2, one needs to differentiate between noise level (NL) and source level (SL) estimates. We have chosen to plot these results on the same scale to show that there is no strong spectral dependence at wind speeds greater than 6 m/s (12 knots). In the case of the Kewley (1990), we observe at the most m = +1/3 between 100-200 Hz.

The Kennedy (1990) experiment was performed with a measurement array of seven octavely nested four wavelength linear apertures covering the 40- to 4000-Hz band. Meteorological measurements were performed on Andros Island. In his experiment, Kennedy was able to model the propagation in the Tongue of the Ocean. Since we know (Talham (1964)) that the vertical distribution of ambient noise $N(\theta)$ can be written as

$$N(\theta) = dI/d\Omega = DPWg(\theta')\exp(-2\alpha r)/\cos\theta'(1-\beta\gamma \exp(-4\alpha r)),$$

where $W = [\sin\theta'/\sin\theta] = [C_s/C_r]^2$,
D = source density at surface (number/m^2),
P = power (watts/sr),
$dI/d\Omega$ = intensity/unit solid angle (watts/m^2/sr),
α = frequency-dependent absorption coefficient,
γ = surface reflection coefficient,
β = reflection coefficient of the bottom,
θ' = source angle,
θ = angle at receiver, and
C_s, C_r = speed of sound at source and receiver,

we see immediately that, given a knowledge of the environmental factors, one could estimate $g(\theta')$ given a measurement of $N(\theta)$. Kennedy measures $N(f,\theta)$ and determines with a similar but more complicated method of curve fitting the best fit to $D \cdot P \cdot g(\theta')$. Kennedy's results are shown in Fig. 2 for a wind speed of 8 m/s (16 knots). These results show a practically white spectral curve. The novel aspect of Kennedy's experiment is his ability to estimate the source directional characteristic $g(\theta')$ as a function of wind speed and frequency. Shown in Fig. 3 are two examples of $N(f,\theta)$ from this estimation based on his measured data. Figure 3A shows the estimated pattern at low wind speeds prior to whitecaps being present. A broad maximum is observed at 600 Hz that is directional. At the lower frequencies, less directionality is observed. Kennedy found that with whitecaps present (Fig. 3B) the vertical directional spectra were consistent with a surface distribution of point dipole sources over the entire frequency range with a broad maximum at 400 Hz.

The structure shown in Fig. 3A can also be modeled by point dipoles near the broad maximum at 600 Hz, but at the lower frequencies (<300 Hz) the structure is consistent with volume-distributed monopole sources or noise from a distance. Thus, Kennedy's results not only show a slowly varying spectrum level with frequency but also a dipole characteristic for sound generated near the sea surface associated with wave breaking.

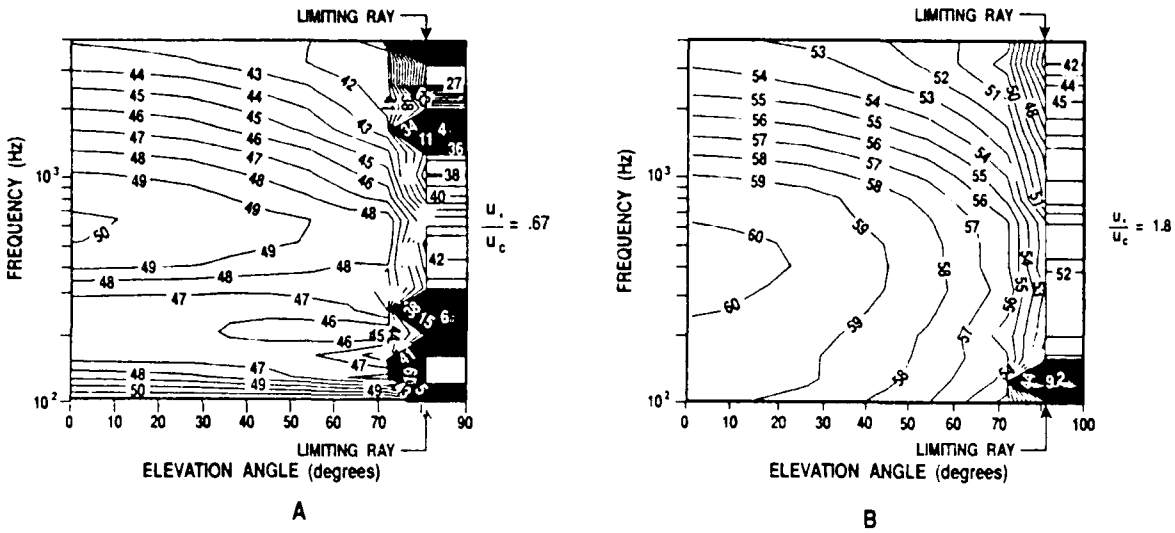

Figure 3. Estimated noise spectrum level vs elevation angle as determined by Kennedy (1990) from comparison of the field from surface distributed dipoles and measured results.

Marrett and Chapman (1989) have performed measurements of low frequency (15 to 250 Hz) ambient noise in the South Fiji Basin with a towed line array. Local wind speed measurements were performed. Shown in Fig. 2 are the 25-knot noise level results. The spectrum again has a fairly white character. For wind speeds greater than 15 knots, the wind speed dependency factor was found to be n≈1.32 at 250 Hz to n≈2.13 at 30 Hz.

These recent deep water ambient noise measurements show that for wind speeds greater than 6 m/s, the sea surface sound has a slowly varying spectral shape with a broad maximum ranging from 300 to 500 Hz. In addition, we are shown in Fig. 2 the results from three shallow water experiments. Ferla and Kuperman (1984) have reported results on the wind generated source spectrum levels for wind speeds between 10 to 40 knots. Ferla and Kuperman used propagation loss measurements and environmental information in a wave theoretic noise model to derive these source levels from measured noise levels. As can be seen, their results are consistent with the deep water curves. Also shown are results from Wille (1984) in the North Sea at 40 to 50 knots and Hollingberger in an Alaskan fjord at 14-15 knots. To obtain the curve attributed to Wille, we have applied an estimated but relative correction factor based on measured propagation loss to their measured noise levels. The results are all similar in shape although different in level.

This characteristic, the broad maximum between 300 to 500 Hz, has been recognized in wind-generated ambient noise for quite some time (Wenz (1962), Piggott (1964)), but not identified with such a diverse set of experiments. The broad maximum that is seen between 300 to 500 Hz in most of the curves shown in Fig. 2 shows a decreasing spectrum level as frequency decreases. This decrease corresponds to a spectral

slope factor of n~1/3 or 1 dB/octave. This characteristic has often been compared to the relative spectrum of noise due to a spray of water droplets developed by Franz (1959). However the Franz spectrum has a steeper (1.3-1.4 dB/active octave) slope than those shown here; nevertheless, the observation of their similarity is worthy of detailed consideration.

2.2 The Low-Frequency Wind Speed Dependency

In the previous discussion of low-frequency noise measurements, we have continually indicated that the wind speed dependency characterized by the factor n(f) has been observed to range from 1.3 to 2.5. Wind speed has traditionally been used to provide an index to the level of noise to be expected at the higher frequencies. But even at high frequencies, the wind speed dependency factor may be variable and complex. To illustrate the complexity of wind speed dependency factor n, we have produced the schematic shown in Fig. 4, which has been adapted from the work of Wille and Geyer (1984). These data were obtained in the North Sea, a region with appreciable shipping-generated noise. The specific data set illustrates what we believe is found in the literature concerning the wind speed dependency. The spectral curve at 20 kHz below a wind speed class of 10 shows no dependency (n=0); between wind speed classes 11 and 13, a dependency of n=2; and at higher wind speeds, a reversal of slope and a decrease in noise level.

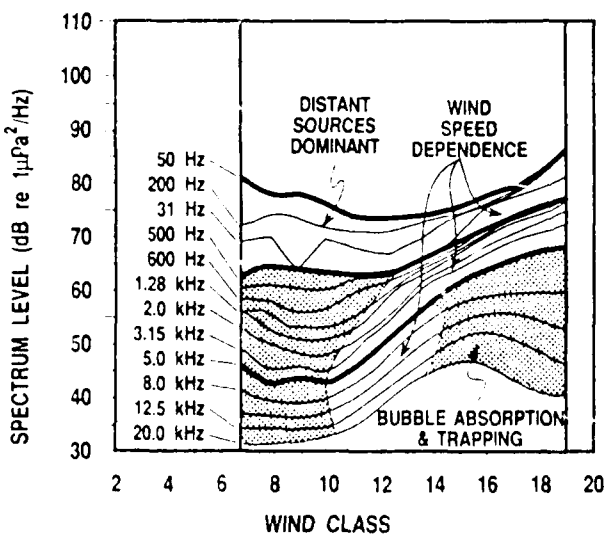

WIND CLASS	WIND SPEED
7	1.6 - 2m/s
8	2 - 2.5m/s
9	2.5 - 3.15
10	3.15 - 4
11	4 - 5
12	5 - 6.25
13	6.25 - 8
14	8 - 10
15	10 - 12.5
16	12.5 - 16
17	16 - 20
18	20 - 25
19	25 - 31.5
20	31.5 - 40

WD = 30m
WSH = 46m

Figure 4. Spectrum level of ambient noise vs wind speed class in the North Sea as measured by Wille (1984). These spectra show the general wind speed dependency of ambient noise.

This trend is seen to persist in some degree down to 5 kHz. The decrease in sound level at wind speeds greater than 10 m/s has been attributed to bubble absorption and sound trapping in the near-surface sound duct produced by sound speed gradients resulting from the presence of microbubbles (Wille and Geyer (1984), Farmer and Vagle (1989)). At

1 kHz we observe a region of no wind speed dependence below a wind speed class of 12 and a wind speed dependency of n=1.75 at greater wind speeds. At lower frequencies, ≈200 Hz, a wind speed dependency is only observed at the higher wind classes (W.C.>16, W.S.>12.5 m/s).

In general what is observed in measurements of wind speed dependence is a noise-limited region, a transition region, and a high wind speed region. These regions are shown in Fig. 5 for representative wind speeds and values of n. Classifying measurements in these regions may aid in the interpretation of low frequency noise levels and explain the variation found in the published values of n(f).

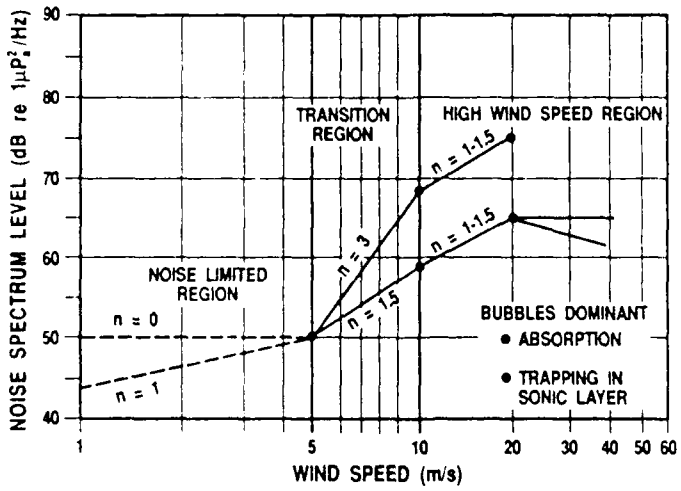

Figure 5. Wind speed dependency (n(f)) vs wind speed for frequency <500 Hz. Three regions are identified, a noise limited region, a transition region, and a high wind speed region.

We have used this scheme to examine the value for n(f) for noise results obtained at wind speeds greater than 6.5 m/s on selected experimental results. The summary of this analysis is shown in Fig. 6 along with the values reported by Crouch and Burt (1972), Piggott (1964), and Marrett and Chapman (1990). It is important to mention that all results were used in our summary curve shown in Fig. 6. The trend is clear for high winds speeds; n(f) has a constant value ~2.5 until a frequency of 50 Hz and ~1.2 value for frequencies greater than 300 Hz. The variation of n(f) with f between 50 and 200 Hz appears to be real. Kerman (1984) has observed that all high frequency results (>500 Hz) yield a consistent set of characteristics. This indicates that sound production at these higher frequencies may be from the same mechanisms, such as bubble, splash, and spray. However, the variation of n(f) at the lower frequencies may indicate a different mechanism.

2.3 Low-Frequency Noise Characteristics

We now have an answer to the question "What are the characteristics of low frequency (<500 Hz) ambient noise?" First, we cited evidence that showed breaking waves produce sound with frequency content as low as 30 Hz. The Hollett spectra appear to be a random collection of spectral

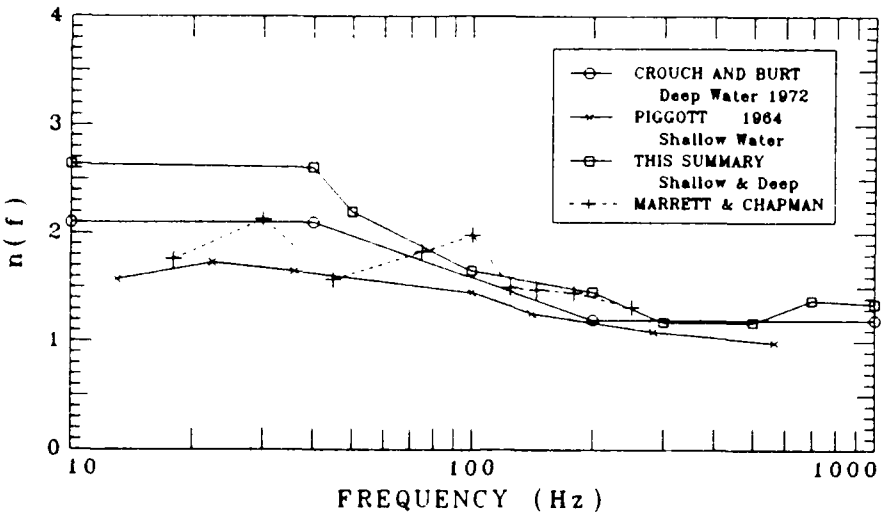

Figure 6. Wind speed dependency factor n(f) vs frequency for wind speeds >13 knots. Shown are the results of Crouch and Burt (1972), Piggott (1964), and Marrett and Chapman (1990) and an average of all data.

peaks spread in frequency and time during the breaking event. These results are similar to those of Farmer (1989), although in some instances Farmer observed a broadband event representative of impact noise at the beginning of the wave breaking, followed by the subsequent random collection of spectral peaks.

Second we showed that measurements of local wind-generated noise at wind speeds greater than 6 m/s have a broad maximum between 300 and 500 Hz. The position of this maximum shifts to lower frequencies as the wind speed increases. The decrease in spectrum level with a decrease in frequency below this broad maximum is less than m=1/3 (1 dB/octave).

Third, we showed that the wind speed dependency (n(f)) of local wind generated noise is a complex function and may be characterized by three regions. In the high wind speed case, the low-frequency noise level (dB re 1 $\mu Pa^2/Hz$) increased with a wind speed dependency n(f)=1.5 at 200 Hz, which ranged between 1.3 at 500 Hz to 2.5 at 30 Hz.

Finally, the results of Kennedy (1990) clearly show that low frequency sound produced at the sea surface after the occurrence of wave breaking has a dipole characteristic. Thus, the problem is reduced to finding a sound-generating mechanism that produces a broadband event followed by a random collection of spectral events, which scale according to $U^{2n(f)}$ power.

2.4 The Whitecap Index

Wilson (1983) proposed that above 200 Hz, the noise levels vary in proportion to the "whitecap" index, W(u), of Ross and Cardone (1979). Wilson proposed three regions of wind speed dependency:

$$\text{I.} \quad W(u) = 0, \qquad u \leq 4.5 \text{ m/s}$$

$$\text{II.} \quad W(u) = (4.6\text{x}10^{-3})U^3 - (4.9\text{x}10^{-2})U^2 + (4.63\text{x}10^{-1})U - 1.5, \qquad 4.5 \leq U \leq 15 \text{ m/s}$$

$$\text{III.} \quad W(u) = (20.97)(U/15)^{1.5}, \qquad 15 \text{ m/s} \leq U .$$

The first region has no whitecaps; the second was attributed to an empirical fit to the data of Ross and Cardone; the third, or high wind speed region, was based on Wilson's analysis of Perrone's data. The speculation put forth by Wilson was the relationship between whitecaps and acoustic noise was in three individual wind speed dependent regions.

We have observed a wind speed dependency of n(200)~1.5, a noise intensity variation of U_{10}^3. However, if low-frequency sound is associated with the breaking waves characterized by the whitecap index, which vary as U_{10}^3, then why does the low-frequency noise level only vary with U_{10}^3 and why is this factor so variable. Kerman (1984) has developed an explanation for the higher frequency wind speed dependence based on bubbles with radii comparable to the Kolmogorov length scale, but this explanation may not apply at these frequencies.

Wu (1980) stated that the whitecap index W(u) should be related to the energy flux of the wind under equilibrium conditions. The energy flux ($\dot{E}$) or the rate of doing work is related to the wind stress (τ) and a surface drift current (V),

$$W(U_{10}) \propto \dot{E} = \tau V \propto \tau U_* \propto C_{10}^{3/2}\, U_{10}^3 ,$$

where $W(U_{10})$ is the percentage of the sea surface covered by white caps, τ is the shear stress at the surface, U_* is the friction velocity, and U_{10} is the 10-meter-elevation wind speed. This relationship between the white cap index and the wind stress coefficient (C_{10}) ties the whitecap index to fundamental parameters governing the exchange of momentum, mass and energy in the sea surface interaction zone.

Kitaigorodskii (1972) outlined the fundamental dependency of the wind stress coefficient on three quantities

$$C(Z,U) = C(Z/h_s, R_i, R_{es}) ,$$

where Z is the observation point, h_s is the characteristic scale of the roughness, R_i is the Richardson number, and R_{es} is the Reynolds number for roughness. Kitaigorodskii shows, for a moving boundary under neutral stability conditions, that

$$U(Z)/U_* \simeq 1/\kappa \ \ln(Z/h_s) = C(Z,U)^{-1/2},$$

where $U_* = \sqrt{(\tau/\rho)}$ is the friction velocity, κ is Von Karman's universal constant and h_s is given by

$$h_s \simeq [2 \int_0^\infty S(\omega)\exp(-2\kappa g/\omega U_*)d\omega]^{1/2}$$

with $S(\omega)$ being the frequency spectrum of the wave field. In general, the wind stress coefficient is dependent on the stability of the boundary layer as well as the roughness scale modified by the motion. Given that the whitecap index is proportional to this quantity to the 3/2 power, we can expect variability.

The whitecap index can be approached by either measuring the index directly or by measuring the wind stress coefficient. Monahan (1990) (see also O'Murcheartaigh and Monahan (1986), Monahan and O'Murcheartaigh (1981)) has determined the wind speed variation of the whitecap index by fitting

$$W(U_{10}) = \alpha U_{10}^{\lambda}$$

to measured fractional whitecap coverage data. Monahan finds that $\lambda = 3.41$ provides the best fit to all data sets, but individual sets of data yielded values of $\underline{\lambda}$ between 2.55 and 3.75. Monahan has also proposed classifying whitecaps as class A, young, and class B, old. Wu(1981,1986) contends that $C(U^{10}) \propto U_{10}^{1/2}$, and consequently a variation of W with $U^{3.75}$. However, Wu (1980) in a revisit to this question recognized the linear dependence of $C(U_{10})$ on wind speed. His review of measurement of the wind stress coefficient as a function of U_{10}^{3m} showed most measured values of m between a value of 1 and 1.3. (Also, see Large (1981), Donelan (1982) and Smith (1980).) The reader is cautioned concerning the use of relationships between the whitecap index and $C(U_{10})$.

Amorocho and De Vries (1980) examined the issue of variability by plotting $C(U_{10})$ and U_* versus U_{10} for a wide range of wind speed conditions. The results of their curve fits are shown in Fig. 7. In general, they find three distinct wind speed regions. The first region is found prior to the onset of breakers with C_{10} constant. The second region, labeled as a transition region, is for wind speeds between 7 and 20 m/s. In this region, both U_* and C_{10} have linear dependencies on wind speed. This region would correspond to $W(u) \propto U_{10}^{4.50}$, which is larger than Monahan's observations. Finally, for wind speeds greater than 20 m/s, a saturation region with C_{10} again constant and an expected variation of $W(U_{10}) \propto U_{10}^{3}$.

These results are remarkably similar to the acoustic noise level characteristics. Since most observations of noise are in the 7- to 20-m/s wind range, we can expect a variation in our wind speed dependency similar to the variation in wind stress coefficient. Since we also expect a dependency of the wind stress coefficient on the Richardson number and the sea state spectrum, ambient noise levels may also be affected. Thus, one may conclude that ambient noise measurements should be performed that concurrently measure the wind speed (U_{10}), the air-water temperature difference as a simplified R_i measure, the sea state spectrum as an indicator of roughness, and the moisture content necessary for correct estimation of R_e.

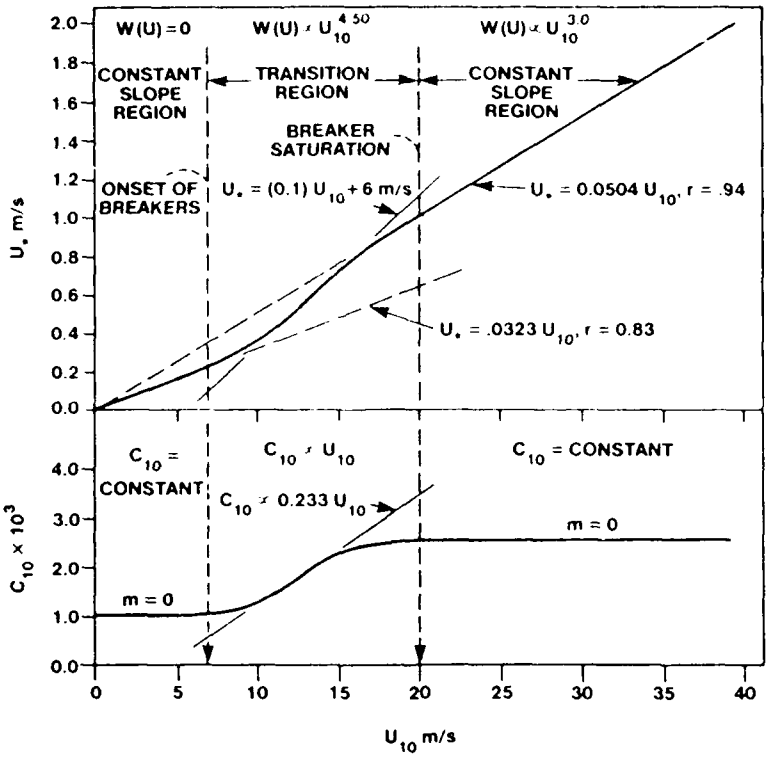

Figure 7. The friction velocity, U_*, and wind stress coefficient, C_{10}, vs wind speed taken from Amorocho and DeVries (1980). These regions are identified as a constant slope region prior to wave breaking, a transition region, and a constant slope after breaker saturation.

3. BREAKING WAVES: BUBBLE PLUMES AND CLOUDS

The association of wave breaking with the production of low frequency sound and subsequently deep ocean ambient noise characteristics leads us to examine bubble production from this wave breaking process. Fresh water laboratory measurements, such as the experiments by Ming-Yang Su (1984) with three-dimensional waves, show a typical sequence of events from the initial wave breaking to the formulation of a columnar bubble plume to a more diffuse cloud swept by the subsurface orbital motion and finally to dispersion of near-surface bubbly features. While fresh water experiments may be useful in visualizing the sequence, the bubbly mixture in these types of experiments appears to be composed of larger bubbles, faster rise times, and consequently different acoustic characteristics. The difference in the bubble sizes and rise times may also result in different sound production mechanisms.

Thorpe (1986,1982) and his colleagues have performed a series of experiments with upward-looking sonars in lakes and in the deep ocean. He observed bubble clouds convected to meter depths initially by wave breaking turbulence and vorticity and subsequently ordered patterns consistent with Langmuir circulation. Thorpe's results show an exponential decrease in volume scatter strength with depth, a mean

depth of penetration that was proportional to U_{10} and the air-water temperature difference ($\Delta\theta_{Aw}$) and finally a different cloud characteristic for stable ($\Delta\theta_{Aw}>0$) and unstable ($\Delta\theta_{Aw}<0$) conditions. For example, the stable condition was found to result in a "billowy" cloud structure, whereas the unstable condition resulted in a columnar characteristic. Recently, observations by Crawford and Farmer (1987) confirmed these effects as well as an exponential distribution of bubble density with an "e folding" depth between 0.7 and 1.5 m, a near-surface bubble density variation with $u_{10}^{3\pm.3}$, a weak dependence on the Langmuir circulation, and "v"-shaped columnar clouds for ($\Delta\theta_{Aw}<0$).

Thorpe also observed pronounced differences in clouds produced by wave breaking in fresh and salt water. Thorpe attributed these differences to chemical effects discussed by Scott (1975) to explain Monahan's (1969, 1971) observation concerning fresh water white caps. That is, under nearly identical physical conditions, bubble distributions produced in salt water have a smaller mean radii and a larger number of bubbles. According to Scott (1986), surface chemical effects can be an important factor preventing coalescence, and "Significant differences observed in fresh water and salt water white caps may be ascribed to these effects, bubbles in salt water being (as a result) greater in number, smaller, more densely packed, carried deeper, and slower to rise to the surface than those formed in fresh water by a similar wave breaking event." Pounder (1986) also showed a distinct temperature-dependent difference between distilled water (coalescence occurs) and salt water (coalescence does not occur). He attributed this difference to ionic effect. However, Pounder's laboratory observations support the conclusion drawn by Scott and Thorpe that microbubble distributions result from salt water wave breaking.

Bubble size measurements (made by Medwin (1977), Kalovayev (1976), Johnson and Cooke (1979), Bouguel (1985), and Crawford (1987) and then reviewed by McDaniel (1987)) yield distributions with most probable bubble radii between 50-70 μm, with an exponential decrease in number with an increase in radii. Kalovayev observed that at wind speeds of 13 m/s, all bubbles were less than 350 μm, although the position of the distribution maxima was observed to shift to larger radii with increasing wind speed and depth.

Recently, Monahan (1990,1987) has developed a hypothetical model for the evolution of a bubble plume and cloud from a breaking wave consistent with the results discussed here. Shown in Fig. 8 are the results of his analysis for a wind speed of 13 m/s. The second panel shows his "β" plume, a bubble size distribution derived from his aerosol generation model, and a bubble size distribution based on the measurements of Johnson and Cooke (1979).

Monahan uses exponential variation in depth, cross sectional area, and time with measured "e folding" characteristics to scale the results for these α, β, and γ plumes. The α plume occurs within 1-2 s of the breaking event and its characteristic depth of 0.5 m and volume fraction (v.f.) of $4\text{-}8\times10^{-2}$ are based on the extrapolated bubble size distribution shown for the β plume. The β plume is estimated to have a duration between 1 and 10 s and a v.f. based on an integrated size distribution of $1\text{-}2\times10^{-4}$.

Third, the characteristic of the cloud has a bubble size distribution consistent with the measurements of Johnson and Cooke and a scaling based on cloud sea surface ocean to white cap area of 25:1. The duration of this feature is estimated to be on the order of 100 s and an average v.f. between 10^{-6} to 10^{-7}. Monahan's estimates, although carefully derived, are still very uncertain and illustrate that the measurement of v.f. is required to characterize the wave breaking process.

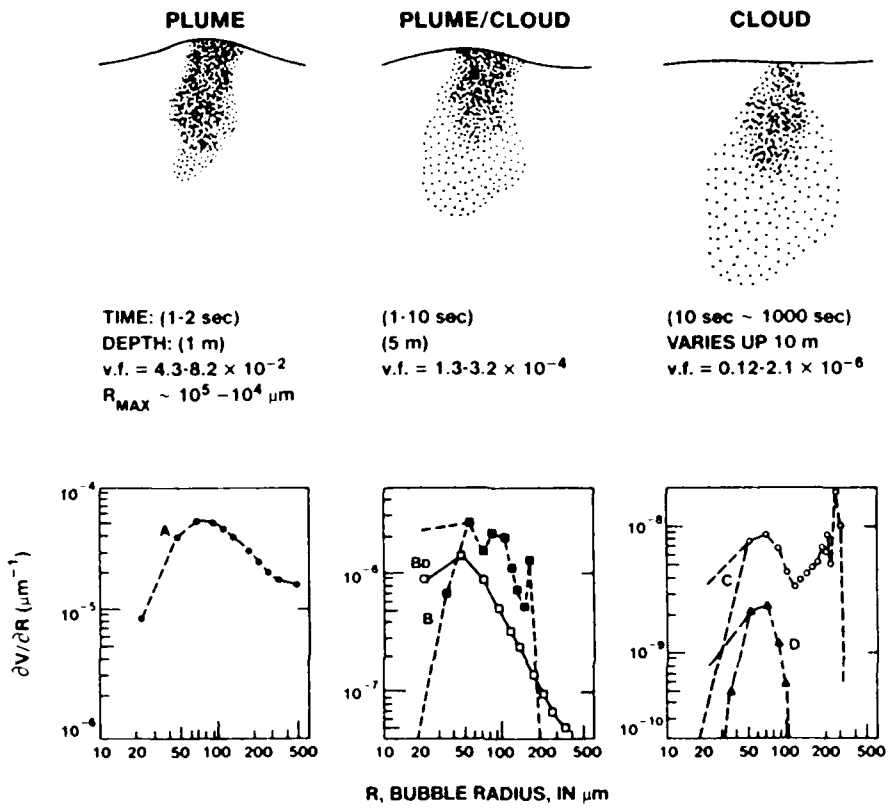

Figure 8. Evolutionary model of a wave breaking bubble plume and cloud shown as a sequence of snapshots covering the time periods of 1 s, 10 s, 100 s. Estimates of v.f. and v.f. distributions are from Monahan (1988).

The measurement of the bubble size distribution, void fraction, and spatial characteristics of bubble clouds and plumes has been shown to be difficult. Nevertheless, general characteristics are beginning to emerge concerning the production of bubbles by breaking waves, the determination of size distribution, and the temporal evolution of these features. Although estimates of the volume fraction as a function of space and time are possible, the direct measurement and knowledge of the volume fraction is still lacking. Laboratory experiments with salt water open-ocean wave generation experiments as proposed by Longuet-Higgins would be useful in determining the single wave breaking plume/cloud void fraction and acoustic characteristics.

4.0 NOISE MECHANISMS

Breaking waves have been observed to produce "impact" noise as well as an ensemble of spectral events. The spectrum measured in the deep ocean has been shown to be fairly white below ~500 Hz and in some respects is similar to the nondimensional spectrum proposed by Franz (1959) to describe higher frequency sound generation by single droplet impact, entrained bubble oscillations and large scale wave breaking events. Prosperetti (1988) has questioned the applicability of this spectrum at the lower frequencies. There is little doubt that at the higher frequencies bubble, spray and splash are primary sources of sound. However, at frequencies <500 Hz, individual bubble and splash sounds are questionable simply on the basis of observed droplet and bubble size distributions.

Nevertheless, just as a single droplet produces an impact and a subsequent entrained bubble oscillation at higher frequencies, a breaking wave may produce a "water hammer" type impact (Nystuen (1986), Paynter (1961)), and a subsequent oscillation of the micro-bubble plume and cloud at lower frequencies. This water hammer effect can be shown to produce a transient pressure pulse with a Fourier spectral amplitude of a dipole, $|P_\omega(R)| \approx \rho U_\omega C \cos\theta / R^2$ where ρ is the density, U_ω the velocity spectrum of the impact, C the sonic velocity, θ the angle from the downward directed normal and R the radial distance. While wave breaking may not produce a truly impulsive event, the resultant average spectrum could resemble Franz's nondimensional spectra. As mentioned by Nystuen (1988), the velocity dependence is linear in this case of a water hammer impact as opposed to the cubic dependence proposed by Fitzpatrick (1959) for solid sphere impacts.

4.1 Mixture Theory

In a bubbly mixture, when the distribution of bubble sizes results in resonant bubble frequencies much greater than the frequencies of interest, then the propagation of sound in the mixture can be described by an effective wave equation with mixture density and sound speed. These effective wave equations have been studied by several investigators (i.e., Foldy (1945), Crighton (1969), Van Wijngaarden (1968)) and confirmed by Karplus (1958) at frequencies <1 kHz. (See Carey (1988).)

A. B. Wood (1932) showed that at low frequencies in an air-water mixture that when the size of the bubbles and spacing between bubbles were small compared to a wave length, that for a given volume fraction (χ) the mixture density (ρ_m) and compressibility (κ_m) are under equilibrium conditions given by

$$\rho_m = (1 - \chi)\rho_\ell + \chi\, \rho_g \text{ and } \kappa_m = (1 - \chi)\kappa_\ell + \chi\, \kappa_g,$$

where ℓ represents the liquid and g the gaseous component. The low frequency limiting sonic speed, C_{mlf}, is seen to be

$$C^2_{mlf} = \frac{dP}{d\rho} = (\rho_m \kappa_m)^{-1}.$$

In the case of the air bubble-water mixture, the process can be considered either adiabatic or isothermal. Since the controlling factor is the rate of heat transfer during bubble compression to the surrounding fluid which is rapid in water due to its large thermal capacity, the bubble oscillations at low frequencies may be considered isothermal. The following equations result:

$$C_{mlf}^{-2} = \frac{(1-\chi)}{C_\ell^2} + \frac{\chi^2}{C^2} + (\chi)(1-\chi)\frac{\rho_g^2 C_g^2 + \rho_\ell^2 C_\ell^2}{\rho_g C_g \rho_\ell C_\ell}$$

$$\chi \to 0 \quad C_m^{-2} \to C_\ell^{-2} \quad \text{and} \quad \chi \to 1 \quad C_m \to \bar{C}_g^2$$

and when $0.002<k<0.94$, $C_{mlf}^2 = P/\rho_\ell \chi(1-\chi)$.

These equations show the large effect on sonic speed as a function of void fraction and relative bulk modulus (Fig. 9). In the low frequency range (<1 kHz) Karplus used an acoustic tube to determine the standing wave pattern as a function of air volume fraction and verified these results. This behavior is due to the mixture's mass being primarily due to the liquid while its compressibility is due to the gas. Since we are dealing with the low frequency response, much less than any individual bubble resonant frequency, only the volume fraction is important and not the bubble size distribution.

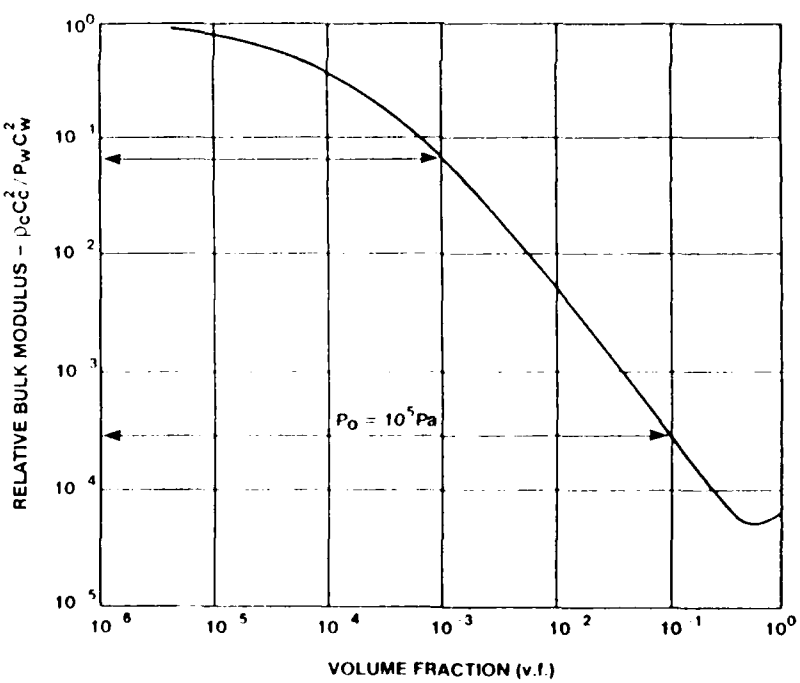

Figure 9. The relative bulk modules versus volume fraction is shown for an air water mixture at a pressure of one atmosphere.

These equations do not show the dispersive nature of this sonic speed variation. If one considers a bubbly liquid with an uniform bubble size whose corresponding resonant frequency is ω_o and dampening δ, then one can solve the component conservation equations to obtain the following frequency dependent sonic speed:

$$\frac{1}{C_m^2} = \frac{(1-x)^2}{C_P^2} + \frac{1}{C_{mlf}^2\,(1 - \omega^2/\omega_o^2 + 2i\delta\omega/\omega_o)}$$

This expression reduces to our previous equation for C_{mlf}^2 when $\omega \ll \omega_o$. The equation does show a dispersive character as illustrated in Fig. 10 compared to the data of Fox (1955). Of interest is the sonic velocimeter range f>240 kHz, $C \to C_l$, the sonic speed of the liquid. The dispersive character of the phase velocity is the reason why volume fraction measurements are necessary to determine the low frequency sound speed changes near the surface of the sea.

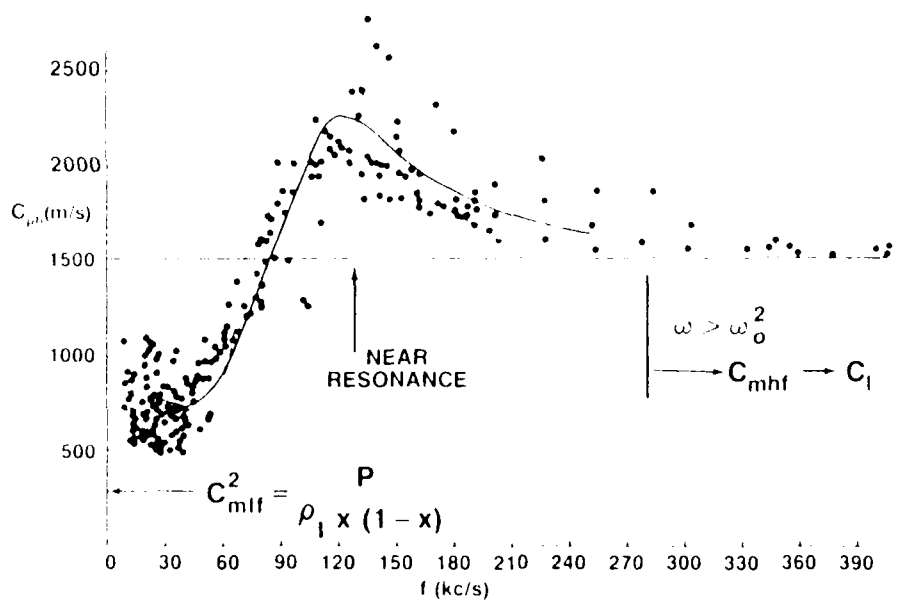

Figure 10. The dispersive behavior of the sonic speed in air water mixtures showing behavior below, at, and above bubble resonance region.

4.2 The Oscillation of a Bubbly Spherical Volume

The generation and scattering of sound from a compliant sphere immersed in a fluid can be found in classical texts on the theory of acoustics (see Reschevkin (1963), or Morse (1948)). In this particular case, the bubbly sphere has no well-defined boundary but nonetheless is localized by perhaps a vortex or some other circulatory feature beneath the breaking wave. Since this analysis is somewhat standard, only a brief outline will be presented.

Here we assume that the bubbly region (Fig. 11) is compact with an arbitrary radius r_o and the region is composed of micro bubbles with resonant frequencies far above the frequency of excitation. Buoyancy

forces and restoring forces such as surface tension are not required. The properties of the bubbly region are described by the mixture speed c and density ρ with a resulting compressibility $1/\rho c^2$. The micro bubbles supply the compressibility and the liquid supplies the inertia.

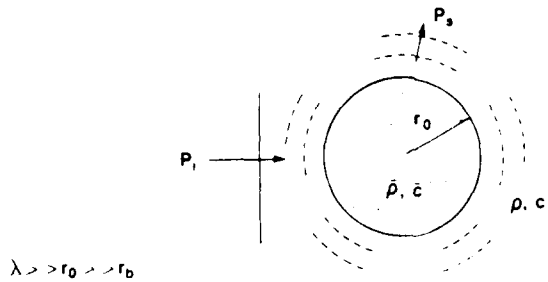

Figure 11. The random collection of micro bubbles within a radii r_o from the origin. (Pi = incoming wave or excitation, $\bar{\rho},\bar{c}$ = the properties of the mixtures, ρ,c = the properties of water, and P_s = the radiated sound.)

The source of excitation is assumed to be global compared to the dimensions of the compact sphere. This assumption means we can assume a plane wave expanded in terms of spherical harmonics. The physical reasoning is that the properties of the bubbly region determine its ability to radiate provided there is a source of excitation, i.e.,

$$P_i = P_o \exp(i\omega t - ikr) = P_o \exp(i\omega t) \sum_{m=0}^{\infty} i^m (2m+1)\, P_m(\theta) J_m(kr). \quad (1)$$

We require continuity of velocity and pressure at the generalized radius, r_o. Furthermore a radiation condition is imposed at large r and the field is required to remain finite within the bubbly region.

The particle velocity $V_i = (-1/i\omega p)\, \partial P_i/\partial r$. (2)

Continuity of Pressure $P_i + p_s = \bar{P}$. (3)

Continuity of Velocity $V_i + V_s = \bar{V}_n$. (4)

The procedure is to assume the scattered wave or radiated wave is a sum of outward propagating spherical waves.

$$P_s = \exp(i\omega t) \sum_{m=0}^{\infty} A_m \bar{P}_m(\theta) G_m(kr) \exp(-i\varepsilon_m kr). \quad (5)$$

The pressure field inside the volume is expanded in terms of spherical Bessel function of the 1st kind, i.e.,

$$\bar{P} = \exp(i\omega t) \sum_{m=0}^{\infty} \bar{A}_m P_m(\theta) J_m(kr). \quad (6)$$

When the region is compact $\lambda > 2\pi r_o$, we can solve for the coefficients A_m and $\bar{A}_m$ by using the boundary conditions (2, 3, and 4) and equating each m order terms. To $O(k^3r^3)$, we find for A_0 and A_1 the following:

$$A_0 = \frac{iP_o(k_o r_o)^3 (1 - y/\bar{y})/3}{[(1 - y/\bar{y} \frac{(kr_o)^2}{3}] - i (kr_o)[y/\bar{y} \frac{(kr_o)^2}{3}]} \tag{7}$$

and

$$A_1 = \frac{P_o(kr_o)^3 (\bar{\rho} - \rho)}{(2\bar{\rho} + \rho)} \tag{8}$$

where $y=\rho C^2$ and $\bar{y}=\rho\bar{C}^2$. The term A_0 is interesting when the real part of the denominator is equal to zero, we may say a resonance has occurred.

This occurs when

$$(kr_o)^2 = (\frac{2\pi f_o r_o}{C})^2 = \frac{3\bar{\rho}\bar{C}^2}{\rho C^2} \quad \text{and} \quad f_o = \frac{C}{2\pi r_o}\sqrt{\frac{3\bar{\rho}\bar{C}^2}{\rho C^2}}, \tag{9}$$

since

$$\bar{C}^2 \simeq \gamma P/\rho_\ell \chi(1-\chi), \qquad f_o = \frac{1}{2\pi r_o}\sqrt{\frac{3\gamma P}{\rho_\ell \chi}}, \tag{10}$$

which we recognize as a modified Minnaert formula for the resonant frequency of a volume oscillation of a gas bubble. (Note that we have inserted a factor γ, the rate of specific heats. This factor applies to individual bubble pulsations and for the cloud we set $\gamma = 1$ corresponding to isothermal conditions.) This result follows because the resonant angular frequency is proportional to the compressibility of the bubbly region, characterized by the stiffness $(4\pi r_o \rho C^2)$ and the inertia $(4\pi r_o^3 \rho/3)$. For the case of air with $C_a \simeq 340$ m/s and $\rho_g/\rho_\ell = 0.0013$, we find the resonant frequency of the gas bubble to be $f_{ob} = 6.758$ Hz-m/2a and for the cloud with a v.f. of $\chi = 0.002$ and $C_m = 200$ m/sec, a resonant frequency $f_{oc} \simeq 110$ Hz-m/$2r_o$. If the average size of each gas bubble is 50 μm, then we have $f_{ob} \simeq 67.6$ kHz, and if the radius of the air cloud is $r_o \simeq 0.25$ m, we find that $f_{oc} \sim 220$ Hz. Thus, the cloud radiates sound at a resonant frequency much lower than its constituents. The dampening is important to mention as we expect dampening constants to exceed the thermal constant at these frequencies due to the dirty nature of sea water bubbles (Eller (1970)).

Shown on Fig. 12 are curves of resonant frequency versus radius of both spherical and cylindrical volumes with bubble v.f. between 10^{-2} and 10^{-3}. These v.f. are consistent with measurements of bubble plumes but must be differentiated from the bubble densities and v.f. within the near surface residual layer.

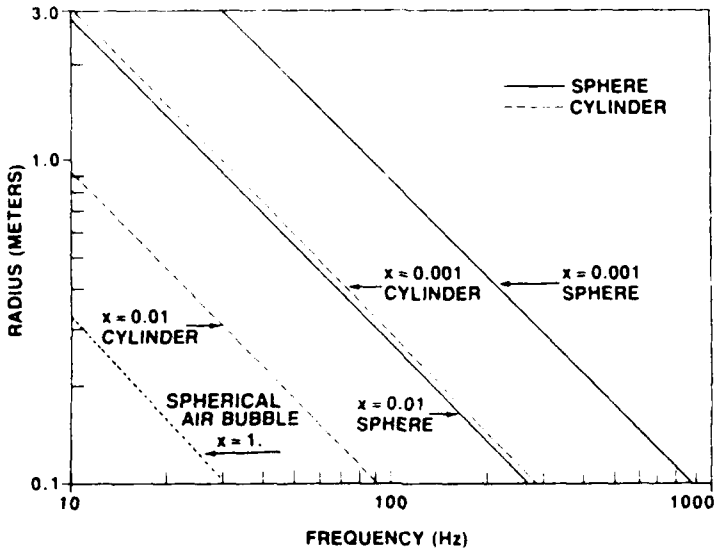

Figure 12. The spherical and cylindrical bubble cloud resonant frequency vs radius and void fraction (v.f.) are shown and compared to a single spherical air bubble.

The curves for the spherical bubble volume are taken from Eqs. (9) and (10) previously derived in this paper. Also shown are curves for a long cylindrical volume. The estimates for the cylindrical volume are scaled by a comparison of the resonant frequency radius at specific void fractions. This ratio of (R_{OS}/R_{OC}) the spherical radius to cylinder radius is shown to be approximately 3. The results show that the frequency radius dependence of a cylinder with a $\chi = 0.001$ corresponds to a spherical cloud of $\chi = 0.01$. These curves show that structures between 10 and 50 cm can have resonant frequencies in our range of interest ~100 Hz. These calculations show that portions of the deep diving bubble plumes have a resonant behavior within the frequency 100 to 200 Hz with reasonable radial sizes.

The result of this analysis is that micro bubble plumes and clouds to first order can be described by compact monopole sources of sound since the radiation from these bubbly regions with an arbitrary boundary has a natural frequency described by the Minnaert formula.

4.3 The Bubble Plume/Cloud as a Compact Source

Minnaert (1933) reasoned that the potential energy accumulated during the compression of a gas bubble to its minimum radius is equal to the kinetic energy of water particles at the time when half the expansion has been reached, returning the bubble to its equilibrium radius. One can perform this type of calculation for either an isothermal or an adiabatic process. For the individual gas bubble, the adiabatic assumption seems appropriate. For the oscillation of a cloud of bubbles, one should use the isothermal assumption due to the thermal capacity of water.

We have shown that a bubble cloud has a first order radiation characteristic of a pulsating monopole source. Following the lead of Strasberg (1956), we represent this by a simple harmonic oscillator equation, i.e.,

$$\ddot{V} + \xi\dot{v} + \omega_0^2 v = 0.$$

We assume that the initial condition is $V(0) = -v_o$ and that the bubble cloud arrived at this condition in an isothermal process. The solution to this problem can be shown as

$$v(t) = -v_o\, e^{-\xi t/2}\, e^{i\omega_d t}$$

and the radiated pressure

$$P(R,t) = \frac{\rho_\ell \ddot{V}(t-R/C)}{4\pi R}\, u(t-R/C).$$

From this expression, we calculate the total energy in the transient event as

$$E = \frac{\rho_\ell}{4\pi C_\ell \eta}\, \omega_{od}^3\, v_o^{\,2} \quad \text{where } \eta = \xi/\omega_{od}.$$

If we have N_B events per unit of time and we choose a reference power corresponding to 1μPa at a distance of 1 m, we find

$$\mathcal{P}/\mathcal{P}_R = \frac{E \cdot N_B \rho_\ell C_\ell}{4\pi(1\mu Pa)^2}.$$

Using our expression for the resonant frequency of the cloud, we find

$$E = \frac{\sqrt{3}}{C_\ell \rho_\ell^{\,1/2} h} \left(\frac{1}{4/3\pi R_o^3}\right) \left[\frac{P}{\chi}\right]^{3/2} v_o^{\,2}$$

$$\mathcal{P}/\mathcal{P}_R = \frac{\sqrt{3}\, N_B \rho_\ell^{\,1/2}}{4\pi h} \cdot \frac{1}{(4/3\pi R_o^3)} \left[\frac{P}{\chi}\right]^{3/2} v_o^{\,2}.$$

We define a source level (SL) as with representative values of all constants at 10^5Pa, i.e.,

$$SL = 10LOG(\mathcal{P}/\mathcal{P}_R) = 10LOG(N_B) + 20LOG(\xi) - 15LOG(\chi) + 80 \text{ dB}.$$

With $v_o = \xi v_o$, $\xi = 10^{-2}$ and $\chi \sim 10^{-4}$ we found

$$SL = 10LOG(N_B) + 76 \text{ dB}.$$

These SL values are large and should be considered as an upper bound.

This value of the monopole source levels needs to be examined with respect to the surface image interference effect. For a monopole beneath the pressure release surface, we may show

$$|P_d(R_o)|^2 = |P_o(R_o)|^2 \{1 + \mu^2 + 2\mu - 4\mu \sin^2(kZ \sin\theta)\}$$

as per the geometry shown in Fig. 13. When the reflection coefficient is taken as $\mu = -1$ and $(Z/\lambda) = kZ < 1$, we find

$$|P_d(R_o)|^2 = |P_o(R_o)|^2 \cdot 16\pi^2 (Z/\lambda)^2 \sin^2\theta.$$

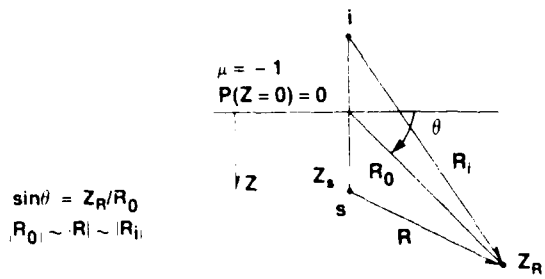

Figure 13. The geometry for the surface image interference is shown with θ taken as π/λ in the downward direction.

This source expression is recognized as a dipole. Integration of this over the half-space one finds

$$\Phi_d = \Phi \cdot (8\pi^2/3)\ (Z/\lambda)^2.$$

Our reference source level now becomes

$$SL = 10LOG(N_B) + 20LOG(\xi) - 15LOG(\chi) + 20LOG(Z/\lambda) + 70\ dB,$$

and with $Z/\lambda \sim 1/15$ we find $SL \sim 10LOG(N_B) + 67$ dB.

Thus, for the case of a bubbly sphere near the ocean surface with $\xi = 10^{-2}$, a volume fraction of $\chi \sim 10^{-4}$, and for a frequency near 100 Hz located at a representative depth below the surface, sufficient source level is achieved. These estimates are uncertain as the knowledge of the dynamic void fraction as a function of depth and time beneath a breaking wave is lacking. However our analysis shows that a plume/cloud can radiate sound with a dipole characteristic and is, thus, a candidate mechanism for the production of sound at low frequencies.

5. SUMMARY, CONCLUSIONS, AND RECOMMENDATIONS

This paper has reviewed data attained at sea that demonstrates that breaking waves are a source of low-frequency (20 to 500 Hz) sound. The experiments reviewed on individual breaking events showed short time (5 s) acoustic signals associated with breaking waves. The spectra

appear to be a random collection of acoustic events in frequency and time. The experiments reviewed concerning deep ocean ambient noise measurements show a fairly white spectrum with a wind dependency n(200)~1.5. However, as we have mentioned experiments that measure not only noise but relevant oceanographic and meteorological factors are lacking. We would recommend that future ambient noise experiments measure not only the 10-meter-wind speed but the air-water temperature difference and the sea surface spectrum. In addition, the sonic velocity variation near the sea surface should be measured especially as one tries to characterize higher frequency noise.

We have suggested that these properties of ambient noise could be explained by wave breaking impact noise (the water hammer effect) and the collective oscillation of bubble plumes and clouds. A key factor in determining the validity of this hypothesis is the time-dependent volume fraction. Since no direct measurements are available concerning this parameter, we must only consider collective oscillations as possible noise sources. This hypothesis could be tested by examining the sound scattering from micro bubble plumes. We have shown that scattering of a plane wave, or excitation of a cloud of bubbles by a coherent source, results in a volume oscillation that is described by Minnaert's formula for the bubbly mixture. Finally, we have attempted to estimate the sound radiation from a cloud of bubbles initially compressed by the wave breaking impact. Levels seem to be adequate to qualify this as a candidate mechanism, but many uncertainties exist and will most likely be determined in future experiments.

ACKNOWLEDGMENT

The authors would like to extend their appreciation for the partial funding of this work to Dr. M. Orr, Code 11250A, of the Office of Naval Research and Dr. K. Lima of the Naval Underwater Systems Center. We would also like to thank our editor, A. C. Mastan (NUSC), for her assistance in preparing this manuscipt.

REFERENCES

Amorocho,J. and DeVies,J.J. (1980) J. Geophys. Res. 85(C1), 433-442.
Bannister,R., Denham,R., Guthrie,K. and Browning D. (1981) J. Acoust. Soc. Am. 69(S1), P595.
Bourquel,M. and Baldy,S. (1985) J. Geophys. Res. 90(C1), 1037-1047.
Burgess,A. and Kewley,D. (1983) J. Acoust. Soc. Am. 73(1), 201-210.
Carey,W.M. and Bradley,M.P. (1985) J. Acoust. Soc. Am. 78(S1).
Carey,W.M. and Browning,D.G. (1988) in Sea Surface Sound, ed. B. R. Kerman, Kluwer Acad. Pub., Boston, 361-376.
Crouch,W. and Burt P. (1972) J. Acoust. Soc. Am. 51(3), 1066-1072.
Crawford,G.B. and Farmer,D.M. (1987) J. Geophys. Res. 92, 8231-8243.
Crighton,D. and Ffowcs Williams,T. (1961) J. Fluid Mech 36(3), 465-474.
Donelan,M.A. (1982) Proc. 1st Conf. of Meteorology and Air Sea Interaction of the Coastal Zone, Am. Meteor. Soc., 381-387.
Eller,A.I. (1970) J. Acoust. Soc. Am. 47(5), 1469-1470.

Farmer,D. and Vagle,S. (1989) J. Acoust. Soc. Am. 86(5), 1897-1908.
Ferla,M.C. and Kuperman,W.A. (1984) SACLANT ASW Res. Ctr Rpt SR-79.
Fitzpatrick, H. and Strasberg, M. (1959) DTMB Rpt 1269, NSRDC/Carderock.
Foldy, L.L. (1945) Phys. Rev. 67(3,4), 107-119.
Fox,F.E., et al. (1955) J. Acoust. Soc. Am. 27(3), 534-539.
Franz,G.J. (1959) J. Acoust. Soc. Am. 31(8), 1080-1096.
Hollett,R. (1988) J. Acoust. Soc. Am. 85(S1), S145.
Hollinberger,D., and Bruder,D. (1990) IEEE J. Oceanic Eng. 15(4).
Johnson,B.D. and Cooke,R.C. (1979) J. Geophys. Res. 84(C7) 3761-3766.
Karplus,H.B. (1958) Armour Res. Foundation, University of Illinois, proj. C00-248-TID4500 (available NTIS, Dept of Commerce, Wash. DC).
Kennedy,R. and Goodnow,T. (1990) IEEE J. Oceanic Eng. 15(4).
Kerman,B. (1984) J. Acoust. Soc. Am. 75(1), 149-164.
Kerman,B. (1988) Sea Surface Sound, Kluwer Acad. Pub., Boston, 361-376.
Kewley,D., Browning,D. and Carey,W. (1990) J. Acoust. Soc. Am.
Knudsen,V., Alford,R. and Emling,J. (1948) J. Marine Res. 7(3), 410-429.
Kitaigarodskii,S.A. (1972), The Physics of Air-Sea Interaction, U.S. Department of Commerce, NTIS., Springfield, VA 22151.
Kolovayev,P.A. (1976) Oceanology 15, 659-661.
Large,W.G. and Pond,S. (1981) J. Phys. Oceano. 11, 324-336.
Marrett,R. and Chapman,N. (1990) IEEE J. Oceanic Eng. 15(4).
McDaniel,S.T. (1987) TM 87-57 ARL/Penn St Univ, State College, PA 16804.
Medwin,H. (1977) J. Geophys. Res. 82(6), 971-976.
Minnaert,M. (1933) Phil. Mag. XVI (7th Series), 235-249.
Monahan,E.C. and Zeitlow,C.R. (1969) J. of Geo. Res. 74, 6961-6966.
Monahan,E.C. (1971) Oceanic White Caps, J. Phys. Oceanogr., 139-144.
Monahan,E.C. and O'Murcheartaigh,I. (1981) J. Physical Ocean. 10.
Monahan,E.C. and MacNiocaill,G. (1986) Oceanic White Caps, D. Reidel Publishing Co., Boston, MA.
Monahan,E.C. (1988) Conf. on Ocean-Atmos. Inter., Amer. Meteor. Soc.
Monahan,E.C. (1988) in Sea Surface Sound, ed. B. Kerman, Kluwer Acad. Pub., Boston, 85-86.
Monahan,E.C. and Lu,M. (1990) IEEE, J. Oceanic Eng. 15(4).
Morse,P.M. (1948) Vibration and Sound, McGraw-Hill, NY.
Nystuen,T.A. (1986) J. Acoust. Soc. Am. 79(4), 972-982.
O'Murcheartaigh,I.G. and Monahan,E.C. (1986) Oceanic Whitecaps, D. Reidel Publishing Co., Boston, MA.
Paynter,H.M. (1961) Handbook of Fluid Dynamics, McGraw-Hill, NY.
Perrone,A. (1969) J. Acoustic. Soc. Am. 46(3), 762-770.
Piggott,C. (1964) J. Acoust. Soc. Am. 36(11), 2152-2163.
Prosperetti,A. (1985) J. Acoust. Soc. Am. 78(S1), S2.
Prosperetti,A. (1988) J. Acoust. Soc. Am. 84(3), 1042-1054.
Prosperetti,A. (1988) in Sea Surface Sound, ed. B. Kerman, Kluwer Acad. Pub., Boston, 151-172.
Reschevkin,S.N. (1963), The Theory of Sound, Pergamon Press, NY.
Scott, J.C. (1975) Sea Res. 22, 653-657.
Scott, J.C. (1986) The Effects of Organic Films on Water Surface Motions in Oceanic White Caps, eds. E.C. Monahan, G. MacNiocall, 159-165, D. Reidel Pub. Co., Boston.
Shooter,J., Demary,T., Wittenborn,A. (1990) IEEE J. Oceanic Eng. 15(4).
Smith,S.D. (1980) J. Phys. Oceano. 10, 709-726.
Strasberg M. (1956) J. Acoust. Soc. Am. Q8(1), 20-26.

Talham,R. (1964) J. Acoust. Soc. Am. 36(8), 1541-1544.
Thorpe,S.A. and Stubbs,A.R. (1979) Nature 279, 403-405.
Thorpe,S.A. and Humphries,P.N. (1980) Nature 283, 463-465.
Thorpe,S.A. (1982), Phil. Trans. R. Soc. Lomd. A304, 155-210.
Thorpe,S.A. (1986) J. Phys. Ocean. 16(8), 1462-1478.
Thorpe,S.A. (1986) Oceanic. White Caps, D. Reidel Publishing Co.,57-68.
Urick,R.J. (1984), Ambient Noise in the Sea, U.S. GPO Washington, DC.
Van Wijngaarden,L. (1968) J. Fluid Mech. 33(3) p. 465-474.
Van Wijngaarden,L. (1980) Caviation and Inhomogenectics, Springer-Verlag, New York, 127-140.
Wenz,G. (1962) J. Acoust. Soc. Am. 34(12), 1936-1955.
Wille,P. and Geyer,D. (1984) J. Acoust. Soc. Am. 75(1), 173-185.
Wilson,J. (1980) J. Acoust. Soc. Am. 68(3), 952-956.
Wittenborn,A. (1976) ADC006902, DTIC, Cameron Station, Alexandria, VA.
Wood,A.B. (1932) A Textbook of Sound, G. Bell and Sons Ltd., London.
Wu,T. (1980) J. Phys. Oceano. 10, 727-740.
Wu,J. (1981) J. Geophys. Res. 86(C1) 457-463.
Wu,T. (1986) Oceanic White Caps, D. Reidel Publishing Co., Boston, MA.

BIBLIOGRAPHY

Axelrod,E., Schoomer,B., and VonWinkle,W. (1965) J. Acoust. Soc. Am. 37(1), 77-83.
Bachman,W. and Williams,R.B. (1975) SACLANT ASW Research Centre Conf. Proceedings No. 17, DTIC, Cameron Station.
Carstensen,E.L. and Foldy,L.L. (1947) J. Acoust. Soc. Am. 19(3) 481-501.
Cato,D. (1976) J. Acoust. Soc. Am. 60(2), 320-328.
Charnock,H. (1955) Royal Meteorological Soc., London, 81, 639-640.
Cipriano,R.J. and Blanchard,D.C. (1981) Bubble and Aerosol Spectra Produced by a Laboratory Breaking Wave.
D'Agostino,L. and Brennen,C.E. (1983) ASME Cavitation and Multiphase Flow Forum, 72-75.
D'Agostino,L. and Brennen,C.E. (1989) J. Fluid Mech. 199, 155-176.
Farmer,D. (1988) ULF/VLF Seismo-Acoustic Noise in the Ocean, Proceedings, G. Sutton, ed., Rondout Assoc., Stone Ridge, NY
Ffowcs Williams,T.E. (1969) Annual Review of Fluid Mech. 1, 197-222.
Fox,G. (1964) J. Acoust. Soc. Am. 36(8), 1537-1540.
Payne,F. (1967) J. Acoust. Soc. Am. 41(5), 1374-1376.
Schippers,I.P. (1980) Rpt 1980-14, Physic. Lab. of National Defense, Res. Org., The Netherlands.
Shang,E. and Anderson,V. (1984) J. Acoustic. Soc. Am. 79(4), 964-971.
Shooter,J. and Gentry,M. (1981) J. Acoust. Soc. Am. 70(6), 1757-1761.
Smith,S.D. (1981) J. Geophys. Res., 86(C5), 4307.
Su,M.Y., Green,A. W., Bergin,N.T. (1984) Gas Transfer at Water Surfaces, Reidel Press, 211-219.
Thorpe,S.A. (1985) Nature 318(6046), 519-522.
Thorpe,S.A. and Hall,A.J. (1987) Nature 328(2), 48-51.
Worley,R., and Walker,R. (1982) J. Acoust. Soc. Am. 71(4), 863-870.
Wu,T. (1985) J. Geophys. Res. 90(C5), 9069-9072.

Appendix

Low Frequency Ocean Ambient Noise: Measurements and Theory

William M. Carey
David G. Browning

A Paper Presented at the
NATO Advanced Research Workshop on Ambient Noise Mechanisms, 15-19 June 1987, La Spezia, Italy

Approved for public release; distribution is unlimited.

TABLE OF CONTENTS

Page

LIST OF ILLUSTRATIONS ii

LIST OF TABLES. ii

INTRODUCTION. 1

EXPERIMENTAL EVIDENCE 2

POSSIBLE MECHANISMS 6

APPENDIX A - DERIVATION OF THE SOURCE INTEGRALS 10

APPENDIX B - MIXTURE THEORY 11

REFERENCES. 14

LIST OF ILLUSTRATIONS

Figure Page

1 Selected Low Frequency Ambient Noise Measurements. 3

2 Ambient Noise Level vs. Frequency for the Witteborn Experiment 3

3 Ambient Noise Spectrum Level vs. Wind Speed, Piggott (1964). . 5

4 Vertical Noise Spectrum Level vs. Angle from the Horizontal, Browning (1986). 6

5. Source Level vs. Frequency and Wind Speed, Kewley (1986) . . . 8

B-1 Low Frequency Approximation for the Mixture Speed 12

B-2 Measured and Computed Mixture Sonic Speeds 13

LIST OF TABLES

Table Page

I Low Frequency Ambient Noise Wind Speed Dependence 4

II Ambient Noise Source Levels. 7

LOW FREQUENCY OCEAN AMBIENT NOISE: MEASUREMENTS AND THEORY

William M. Carey and David Browning
Naval Underwater Systems Center
New London, CT, USA 06320

ABSTRACT. Low frequency ocean ambient noise data are reviewed and summarized. The experimental data, both omnidirectional and directional, when not dominated by shipping noise, are shown to suggest wind dependent noise at the low frequencies (<500 Hz). Candidate mechanisms are examined with the result that wave-turbulence interaction at low sea states and collective bubble oscillations at high sea states are identified as possible sources of this sound. A description of the sonic properties of bubbly water is presented for low void fractions consistent with those observed in bubble clouds and plumes produced by breaking waves. A description of the collective bubble-water mixture as the resonant oscillation of a flexible volume with a sonic speed determined by the properties of the mixture is presented.

INTRODUCTION

The interaction of the wind with the ocean surface has long been recognized as a major source of acoustic noise (Knudsen (1948), Wenz (1962)). Measurements of the omnidirectional noise at the higher frequencies (>200 Hz) have been found to exhibit wind-dependent characteristics; and, when not dominated by shipping noise, the most likely mechanisms are related to bubbles, spray, and splashes associated with white caps, as well as capillary wave/wave interactions (Urick (1984)). Furduev (1966) has proposed that the characteristic broad maxima in the ocean ambient noise spectrum between 0.2 kHz and 1 kHz be attributed to cavitating bubbles. Kerman (1984) discusses these mechanisms in detail (also see Fitzpatrick (1959)), but stresses the noise generated by the non-resonant oscillation of entrained gas bubbles which result from wave breaking and which are forced by intense velocity of the gravity-capillary waves. For wind speeds with a friction velocity greater than this critical velocity, Kerman concludes that sound is produced with a velocity to the 3/2 power, frequency to the -2 power, and intensity proportional to the number of bubbles. However, in the absence of white caps, since noise persists, capillary wave/wave or non-linear wave interactions may be important (Mellen (1987), Kuo (1968)).

At the other extreme of the spectrum (<2-5 Hz), ambient noise associated with ocean microseisms dominates. Recently, this noise has been

shown by Nichols (1981) and by Kibblewhite and Ewans (1984) to be due to wave/wave interaction. The microseismic effect was postulated by Longuet-Higgins (1950) and confirmed by several authors, including Latham and Nowroozi (1968). Several authors have studied the generation of sound through the second-order pressure effect (Brekhovskikh (1967), Goncharov (1970), Hughes (1976), Lloyd (1981)). Kibblewhite and Evans concludes with theoretical arguments and measurements that the dominant noise source in the 0.1 to 5 Hz range is the non-linear wave interaction. Although difficulties were found in predicting absolute levels, both data and theory showed a frequency dependence to the -6 power.

In the very low frequency (VLF, 2-20 Hz) and low frequency (LF, 20-200 Hz), signals from surface shipping are a significant contributor to the measured noise and have been observed to extend to 500 Hz. In this region, noise contributors can be a great distance from the observation point, and consequently the noise field exhibits the effects of sound propagation in both the horizontal and vertical directions (Carey (1986), Von Winkle (1985)). Wagstaff (1981) showed that, if one knows the locations and types of ships, then one can describe the characteristic of the horizontal noise field. Although the vertical noise distribution, including the broad horizontal maxima, could be qualitatively explained, several discrepancies were observed. Wind-driven noise could explain these differences, and the sources of this noise are the subject of this paper.

EXPERIMENTAL EVIDENCE

Omnidirectional noise data at low frequencies which are free from flow and flow-induced vibrations (Strasberg (1984)) are very difficult to obtain. Several investigators (figure 1) measured the spectrum between 2 Hz and 2000 Hz in the deep sound channel or near the bottom. However, most of this data from the relatively heavily trafficked northern hemisphere reflect distant shipping noise in the 2 to 200 Hz range and, consequently, little local wind speed dependence is observed such as shown in figure 1. VLF/LF ambient noise experiments must be carefully examined to ensure that the results are either from distant or local sources.

Wittenborn (1976) (figure 2) performed an experiment with hydrophones that spanned the water column. Hydrophones within the sound channel showed little dependence on local wind speed between 10 Hz and 200 Hz. However, the hydrophone below critical depth showed an inferred local wind speed dependence (10 to 500 Hz) for wind speeds between 5 and 15 kns with levels of 47 dB and 56 dB re 1μPa @10 Hz. The 15 kn spectra showed a slowly varying broad band characteristic between 56 dB at 10 Hz and 65 dB at 500 Hz ($f^{1/2}$). Wittenborn cites an earlier experiment with noise levels of 69 dB for 300 Hz at 30 kns, compared to the 300 Hz levels of 44 dB at 5 kns, 51 dB at 10 kns, and 63 dB at 15 kns. These results suggest two wind noise mechanisms for the cases of low and high sea states with the intensity having a squared velocity dependence (U^2). The abrupt transition between 10 and 15 kns ($U^{6.8}$, based on the levels at 10 and 15 kns and not considered a true velocity dependence), as shown in figure 2, may be a threshold characteristic associated with

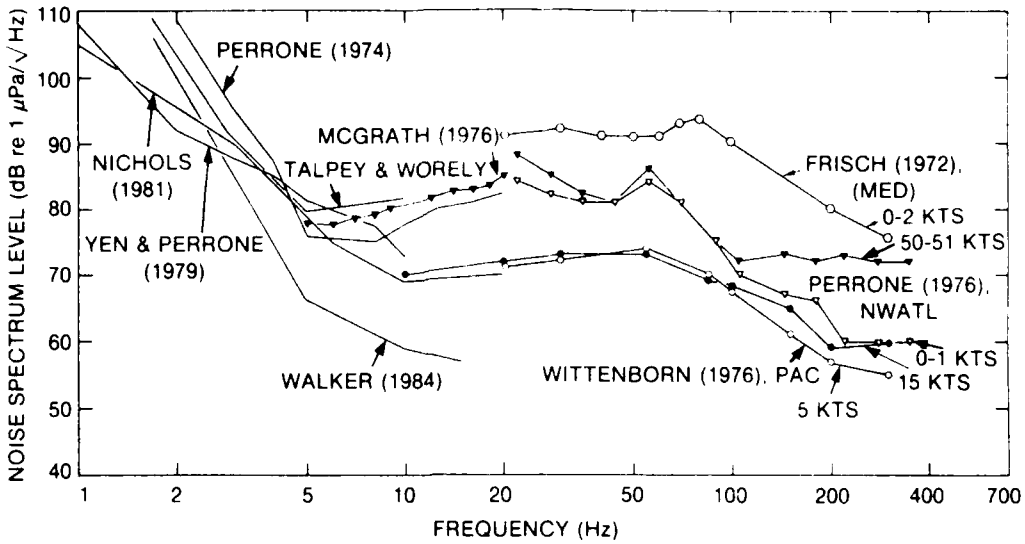

Figure 1. Selected Low Frequency Ambient Noise Measurements. The region less than 5 Hz is dominated by wave/wave interaction. The measurements between 5 Hz and 300 Hz show little local wind speed dependence, but, rather, the effects of distant shipping and other distant noise sources.

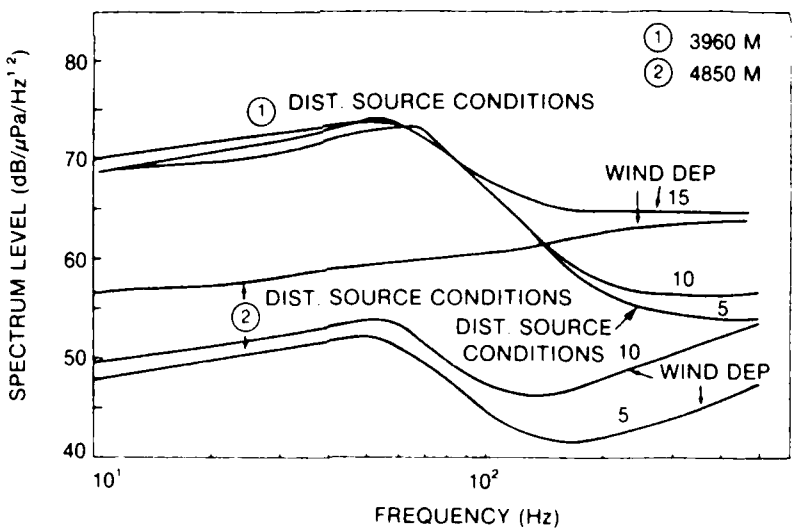

Figure 2. Ambient Noise Level vs. Frequency for the Wittenborn Experiment. The 4850 m deep hydrophone shows the local wind speed dependence (≈200 Hz) with the influence of distant noise sources less than 100 Hz. The 3960 m deep hydrophone is dominated by distant noise sources less 100 Hz.

breaking waves. (These results agree with the observations of Worley (1982), insofar as his data show a threshold-type behavior between the

$NL = NL_1 + 20n\,LOG(W.S.)$

INVESTIGATOR	f	n	w.s.(m/sec.)
PIGGOTT JASA 36(11)	13 13 141 < 50	2.1 0 1.53 2.1	10-20 1-5 3.5-20
PAYNE JASA (1967)	50-100	2.2	
WHITTENBORN (1976)	200-300	1.65 3.4 1	2.5-5 5-7.5 7.5-15
CROUCH JASA 3(2)-72	11 28	1.73 2.09	5-20
SHOOTER JASA 73(6)-81	141 150 177	1-1.39 1.1-1.32 1.36/1.57/.81	5-10 10-15
WORLEY JASA 71(4)-82	100 200	.85-1.5 1.65-2.0	10-15 5-10
WILSON JASA 73(1)-83	10	2.07	5-10
BURGESS JASA 73(1)-83	37	1.66	5-15

FACTORS AFFECTING WIND SPEED DEPENDENCE ARE 1. DISTANT SOURCES; 2. OVERLAPPING WIND SPEED REGIONS. 3. SOUND PROPAGATION FACTORS

Table I. Low Frequency Ambient Noise Wind Speed Dependence

data corresponding to wind speeds between 2.5 and 5 kns and between 5 and 10 kns at 200 Hz. This effect was especially pronounced at 400 Hz.)

Although Wittenborn made use of both refractive effects and bathymetric blockage, noise from distant sources was still found to influence his results (for example, see figure 2 between 10 and 100 Hz). The corrupting influence of distant noise sources (ships, whales, volcanoes, etc.) has the effect of obscuring the low-frequency local wind speed dependence. Consequently, the literature reveals a variety of estimated wind speed dependencies; i.e., the estimate of a parameter n, where $NL = NL_1 + 20\,n \log (W.S.)$. (The mean square pressure would increase with $2n^1$ power of wind speed.) Table I lists several of these estimates of n, ranging from 0.85 to 2.0 for wind speeds between 10 and 20 m/sec. The problem with these estimates also lies in the fact that the data clearly show a region of no wind dependence, a threshold-type behavior, and region with a wind dependence of $n \approx 2.0$.

Figure 3 illustrates this trend with the data of Piggott (1964). One observes the frequency dependent cross-over between the low wind speed and higher winds regions. Furthermore, the lower the frequency, the higher the wind speed will be at which the wind speed dependence point is observed.

Distant noise sources influence vertical noise directionality (Von Winkle (1985), Browning (1982), Bannister (1986)). This influence of the distant source produces a broad maximum in the vertical noise intensity centered on the horizontal. This phenomenon results from the con-

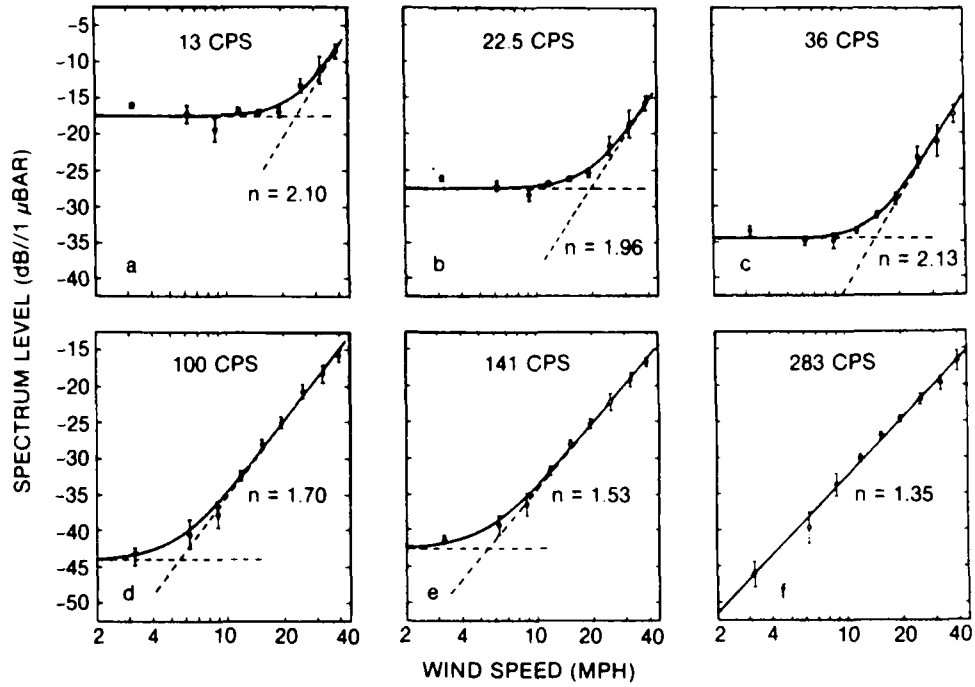

Figure 3. Ambient Noise Spectrum Level vs. Wind Speed, Piggott (1964)

version of higher angle rays to lower angle rays by either reflections from the basin boundaries and seamounts or refractive effects due to shallowing sound channels at the higher latitudes. Wagstaff attributed this effect to surface ships. Since the spectral variation of the horizontal noise is generally smooth, and since ship signatures are narrowband in this frequency range, wind-produced noise over seamounts, slopes, and at high latitudes was speculated to be an important contributor. The broad maximum along the horizontal has been observed in varied geographical locations, such as the sparsely shipped Southern Hemisphere waters of the South Fiji Basin (shown in figure 4). At the lower frequency the data clearly show a broad maximum. At 105 Hz one observes the influence of a single ship. These results are similar to data obtained in the North Pacific and the North Atlantic (Carey (1986)).

The experimental data were examined to obtain measured levels useful in the estimation of the source level of wind-produced noise at the sea surface. These results are shown in Table II, primarily at 50 Hz. The estimated levels based in the Wittenborn data are shown in the table to be between 43 dB at 5 kns and 51 dB at 15 kns, consistent with the estimates by Wilson and Kewley using the same data. Vertical noise cannot be used for local wind-driven noise; however, estimates for a cylindrical basin with sloping sides yields levels in the 50 dB range. Kewley has carefully estimated source levels, and his curves are shown in figure 5.

In summary, we have presented data which indicate the presence of a wind-driven noise in the 10 to 200 Hz region of the spectrum. The low wind speed range (<8-10 m/sec) appears to have a weak dependence on the wind speed, $0 < n < 1$; the high wind speed region (>7.5 to 15 m/sec) appears to have a dependence of $0.85 < n < 2$. These estimates point to

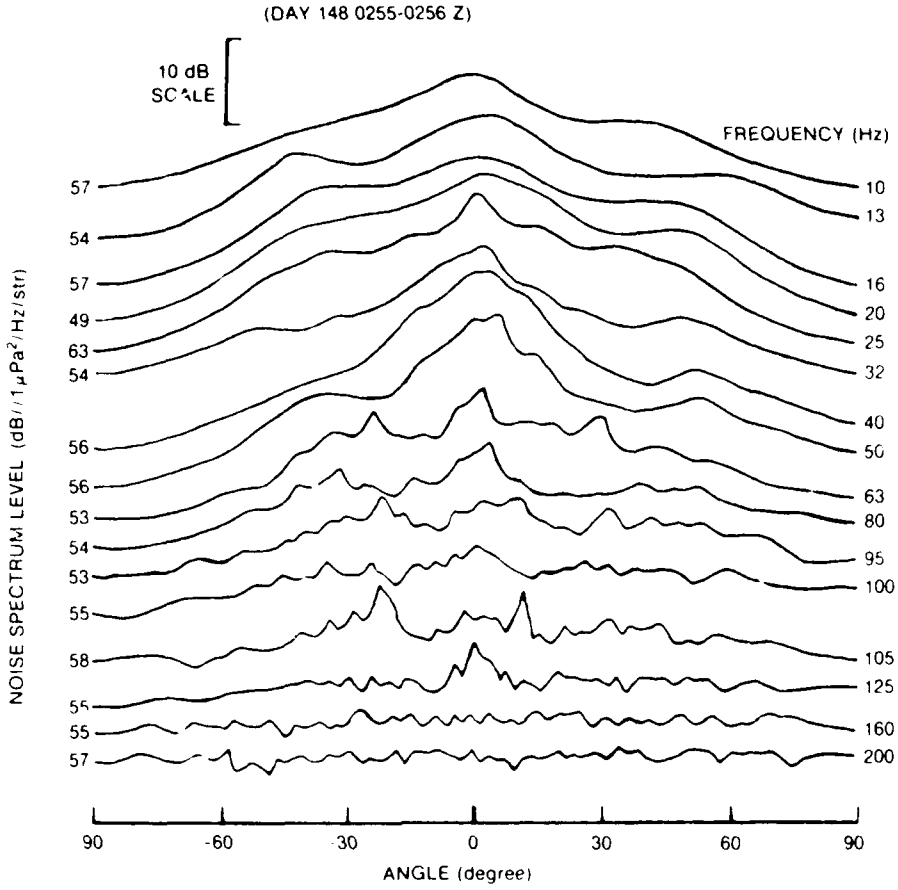

Figure 4. Vertical Noise Spectrum Level versus Angle from the Horizontal, Browning (1986)

the uncertainty in our knowledge of wind speed dependence and spectral characteristics.

POSSIBLE MECHANISMS

The fundamental mechanisms for the production of sound in turbulent regions may be derived from first principles. The basic procedure can be found in several treatments on hydrodynamic noise, most notably Lighthill (1979), Ffowcs Williams (1969), Dowling (1983), and Ross (1976). We have rederived the inhomogeneous wave equation with source terms in appendix A for the purpose of ranking the various mechanisms capable of the production of sound at the surface of the sea in the 10 to 200 Hz range. The basic approach is to write the equations governing the conservation of mass and momentum with source terms. The equation of state is specified, fluctuation quantities assumed, linearization employed, and the inhomogeneous wave equation is formed. The integral solutions to this equation are formulated by use of the Kirchoff Method (Stratton (1941), Jackson (1962)) and of the divergence theorem. The derivation

- OMNIDIRECTIONAL MEASUREMENTS WITH HYDROPHONE BELOW CRITICAL DEPTH:

INVESTIGATOR/FREQ.	10 Hz	50 Hz	100 Hz	w.s.(kns)	
WHITTENBORNE (1982)	48 dB*	50	44	5	N.E. PACIFIC
	50	51	47	10	
	57	58	60	15	
MORRIS (1978)	—	70	63	10	N.E. PACIFIC

- VERTICAL NOISE MEASUREMENTS ALONG THE HORIZONTAL:

INVESTIGATOR/FREQ.	50 Hz	70-80 Hz	100 Hz	
BROWNING (1982)	67 dB	70	65	FIJI BASIN
WAGSTAFF (1981)	—	—	69-66	N.E. PACIFIC
WALES (1981)	95	87	82	N.W. ATLANTIC
AXELROD (1965)	—	—	65-69	N.W. ATLANTIC
FOX (1964)	—	—	60-65	N.W. ATLANTIC
FISHER (1986)	74	—	60	E. PACIFIC
ANDERSON (1979)	—	—	65-69	N. PACIFIC

* dB//(uPa^2/Hz)

- SEMI-EMPIRICAL ESTIMATES:

WILSON (1983) NL=50dB+30LOG(W.S.) @ 50 Hz
BURGESS & KEWLEY (1983) NL=37.3 +15LOG(W.S.) @ 50 Hz

- SOURCE LEVEL ESTIMATES BASED ON OMNI MEASUREMENTS:

f = 10 Hz 41 (dB//uPa••2/Hz @ 1m)@ 5 kns; 50 dB @ 15 kns
50 Hz 43 dB @ 5 kns 51 dB @ 15 kns
100 Hz 37 dB @ 5 kns 56 dB @ 15 kns

- VERTICAL LEVELS YIELD FOR A MEAN WIND SPEED OF 10kns, 50dB@50Hz AND 54-56dB@100Hz

Table II. Ambient Noise Source Levels

in appendix A is similar to those of Huon-Li (1981) and Yen (1979), and the basic result is the following:

$$4\pi C_0^2(\rho-\rho_0) = 4\pi P = \int [\partial q/\partial t]dV/R - \partial/\partial x_i \int [F_i]\, dV/R + \frac{\partial^2}{\partial x_i \partial x_j} \int [T_{ij}]\, dV/R -$$

$$- \int l_i[\partial \rho U_i/\partial t]\, dS + \partial/\partial x_i \int l_i[2\rho_0 U_i u_j + \rho_0 u_i u_j + P_{ij}]\, \frac{dS}{R} \quad .$$

The first term, $\int [\partial q/\partial t]\, dV/R$, represents a monopole term. q represents mass addition rate per unit volume. The second term represents an external force acting on the volume and has a dipole character. These two terms could be important in the incorporation of entrained bubble oscillation and translation. The third term is the Lighthill turbulence stress tensor and is known to represent an acoustic quadrupole. The term $\int l_i[\partial \rho U_i/\partial t]\, dS$ involves the motion of the boundary and can act as a monopole. The final integral involves the turbulent and compressive stresses acting on the boundary and is seen to have a dipole character. In particular the term $\partial/\partial x_i \int l_i[2\rho_0 U_i u_j]\, dS/R$ represents the wave turbulence interaction and is dominant since it represents a product of a first order U_i ; and second order term u_j .

Noise generation by the interaction of surface waves and turbulence near the surface was suggested by Goncharov (1970). He calculated levels of 80 dB at 10 Hz and 40 dB at 100 Hz by assuming a Pierson-Moskowitz surface wave spectrum and Kolmogorov's similarity hypothesis. His expression can be shown to be equivalent to the above integral. However, instead of using velocities, he employs the displacement spectrum for the surface wave and turbulence. His expression is $p(\omega) \sim 40\pi^2/\omega^2$.

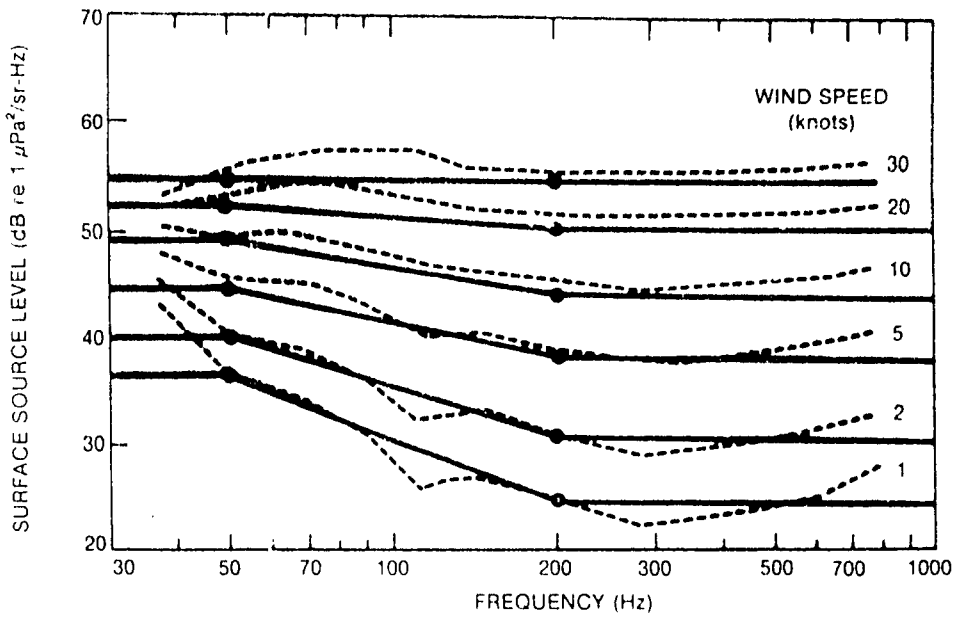

Figure 5. Source Level vs. Frequency and Wind Speed, Kewley (1986)

Yen and Perrone (1979) derived expressions yielding the frequency-dependent radiation characteristics for the wave/wave, wind/turbulence, and wave/turbulence interaction mechanisms. Their results for the wave/turbulence interaction (70 dB at 10 Hz and 50 dB at 100 Hz) show a linear dependence on surface wave velocity (U) and an inverse square dependence on frequency (ω^{-2}) :

$$P(\omega,k) \approx 2 \cdot 10^{-2}\, \rho^2 \cos^4\theta \cdot U/\omega^2 \ .$$

The Yen & Perrone result contains three interesting factors. The linear dependence on surface wave velocity is consistent with the previously discussed experimental results prior to wave breaking. The ω^{-2} dependence is also consistent with the observed behavior at low frequencies; i.e., an overlap region composed of the interaction of the low and higher frequency roll-offs. However, of particular note is the $\cos^4\theta$ dependence. This sharply peaked angular dependence would accentuate the role of the ocean bottom and basin boundaries with respect to the vertical noise directionality. Thus, wave/turbulence interaction could be a source of noise in the 2 to 200 Hz region for those sea states low enough that breaking waves do not occur, due to the fact that it appears as a physically realizable mechanism (considering the uncertainty of the turbulence spectrum).

Kerman (1984) shows that, above a critical wind speed of approximately 10 m/s, small (micrometer (μm)) bubbles are produced and can be a source of higher frequency sound. Thorpe (1986, 1982) has performed interesting experiments which demonstrate the existence of bubble plumes and layers composed of μm-size bubbles (mean bubble size approximately 50 μm with densities between 10^4 to 10^6 bubbles/m^3) extending several

meters below the surface. M.Y. Su (1984) has shown that fresh water breaking waves produced in wave tanks produce bubble plumes which penetrate to depths on the order of signicant wave height, with bubbles of centimeter diameters due to coalesence (which is absent in salt water). Several reviews (see bubble references) have been written on the existence and densities of bubbles produced by breaking waves. At high sea states a residual layer is formed of micro-bubbles with a density that decreases exponentially with depth, and bubble plumes which are convected to several meters depth by the vorticity beneath the wave. Even though individual bubble oscillations with these micron-size bubbles could not produce VLF/LF noise, collective oscillations of the bubbly mixture driven by the hydrodynamic pressure field could produce sound.

It is well known (see appendix B) that a small amount of bubbles in water significantly changes the bulk compressibility while not drastically changing the density. Wood has shown that the sonic velocity (Cm) can be described by the following relationship between void friction (x), density (ρm), and bulk compressibilites (K):

$$C_m^2 = [(1-x)\,\rho_l + x\rho_g][(1-x)\,K + xK_g]\,.$$

The consequence of this result is shown in the figures of appendix B. Small volume fractions result in large changes in the sonic speed when the mixture can be treated as a continuum. For example, the sonic velocity of the bubble mixture with a 0.2% volume fraction is approximately 225 m/s. Ffowcs Williams (1969) describes the efficiency of the radiation from a cloud of bubbly turbulent flow:

$$4\pi C_0^2(\rho-\rho_0) = 4\pi P = \int [\partial q/\partial t]\, dV/R\,.$$

For a compact source with a small gas volume fraction

$$4\pi C_0^2(\rho-\rho_0) = 4\pi P = \frac{1}{R}\frac{\partial}{\partial t}\int q\, dV,$$

Ffowcs Williams estimates that

$$q = -\rho\frac{D}{Dt}\ln(1-x) \rightarrow -C_m^{-2}\, DP/Dt$$

$$dp = C_m^2\,\Delta(1-x)\rho = -\rho C_m^2\,\Delta x \rightarrow \rho-\rho_0 \sim (\rho/R)\, m^4\,(C_0/C_m)^2,\; m = u/C_0$$

Thus he concludes that "a cloud of bubbly flow radiates very much more efficiently than turbulence alone;" that is, the radiation from such a flow would be $(C/Cm)^4 \approx 1975$-times larger than the radiation from turbulent flow. However, one must account for the presence of a pressure release surface.

An alternative approach is to consider the bubble cloud as a flexible sphere of radius a with composite mixture properties and to assume it is compact with respect to the acoustic wave length and the vorticity and turbulence scales. Then the forced oscillation of the bubble cloud in absence of a boundary is $t' = t-R/C_0$, $Q = \int q\, dV = \frac{d}{dt}(\rho_0 v)$

$$P(R,t) = \dot{Q}(t')/4\pi R = \rho_0\frac{\ddot{V}(t)}{4\pi R} = \frac{3\omega^2 a^3\rho}{(1-x)}\, m^2(C_0^2/C_m^2)\, f(\omega)/R,$$

where f(w) represents the simple harmonic oscillator transfer function. This forced oscillation of a bubble cloud can have a resonant behavior

(Fitzgerald and Mellen (1982)). The bubble cloud is simply a monopole source and the presence of the boundary can be approximately taken into account via the surface image interference effect. Thus, we find the following for a cloud of micro-bubbles below the pressure release surface driven in forced oscillation by the hydrodynamic forces:

$$|p(R,t)|^2 \cong \left[\frac{3\omega^2 a^3 \rho}{(1-x)} m^2 (C_0/C_m)^2 f(\omega) \right]^2 \frac{4}{R^2} \left(\frac{2\pi z}{\lambda} \right)^2 \sin^2\theta \, .$$

This expression shows a frequency-dependent efficiency approximately $(z/\lambda)^2$ at a given bubble cloud depth. This term indicates that, as seas pick up, the deeper the plume, the more efficient the radiation at longer λ. Furthermore, we note that this monopole has an m^2 improvement over the non-compact bubble cloud.

Thus, the low-frequency noise could be caused by wave turbulence prior to wave-breaking and, thereafter, by aggregate bubble (bubble cloud) oscillations exhibiting a threshold-type behavior and velocity squared dependence for the mean radiated pressure.

APPENDIX A: DERIVATION OF THE SOURCE INTEGRALS

The purpose of this appendix is to briefly outline the derivation of source terms important to the production of sound near the surface of the sea.

Conservation of mass: $\partial\rho'/\partial t + \partial\rho' v_i/\partial x_i = q$.

Conservation of momentum: $\dfrac{\partial\rho' v_i'}{\partial t} + \dfrac{\partial\rho' v_i v_j}{\partial x_i} = -\dfrac{\partial P'_{ij}}{\partial x_j} + F_{ei}$,

where $P'_{ij} = -p'\delta_{ij} + \mu D_{ij} + \mu_i \Theta \delta_{ij}$ (ref. Hinze, p. 17)

$$\mu_i = 2/3\mu, \; D_{ij} = \partial U_i/\partial x_j + \partial U_j/\partial x_i \text{ and } \Theta = 1/2 D_{ii} = \partial U_k/\partial x_k \; .$$

Taking $\partial/\partial t$ of the continuity equation and $\partial/\partial x_i$ of the momentum equation yields upon subtraction:

$$\partial^2 p'/\partial t^2 = \frac{\partial^2 \rho' v_i v_j}{\partial x_i \, \partial x_j} + \frac{\partial^2 P'_{ij}}{\partial x_i \, \partial x_j} - \frac{\partial F_{ei}}{\partial x_i} + \frac{\partial q}{\partial t}$$

$$v = U + u, \; (\partial U/\partial x_i = 0), \; p' = p_0 + p, \; \frac{\partial p_0}{\partial t} = \frac{\partial p_0}{\partial x_i} = 0$$

$$\partial^2 p/\partial t^2 - C_0^2 \, \partial^2 p/\partial x_i^2 = U_i U_j \, \partial^2 p/\partial x_i \, \partial x_j +$$

$$+ \frac{\partial^2 (p_0 + p) u_i u_j}{\partial x_i \, \partial x_j} + \frac{2\partial^2 (p_0 + p) U_i u_i}{\partial x_i \, \partial x_j} -$$

$$- \frac{\partial C_0^2 p \delta_{ij}}{\partial x_i \, \partial x_j} + \frac{\partial P_{ij}}{\partial x_i \, \partial x_j} - \frac{\partial F_{ei}}{\partial x_i} + \frac{\partial q}{\partial t} \; .$$

For the case of incompressible, invisid flow with no sources or sinks:

$$\partial^2 \rho_0 u_i u_j / \partial x_i \partial x_j + 2 \frac{\partial^2 \rho_0 U_i u_j}{\partial x_i \partial x_j} + \partial^2 p / \partial x_i^2 = 0 \; ;$$

Compressible fluid:

$$\rho C_0^2 = P$$

$$1/C^2 \, \partial^2 P/\partial t^2 - \partial^2 P/\partial x_i^2 = \partial q/\partial t - \partial f_{ei}/\partial x + \partial^2 T_{ij}/\partial x_i \partial x_j$$

$$T_{ij} = 2\rho_0 U_i u_j + \rho_0 u_i u_j + P_{ij} - C_0^2 \rho \delta_{ij} \quad ;$$

(in most instances $P_{ij} - C_0^2 \rho \delta_{ij} = 0$, (Lighthill)).

Since $P = \rho_0 \, \partial\psi/\partial t = -i\omega \rho_0 \psi$, we finally have the wave equation with the source terms:

$$\frac{\partial^2 \psi}{\partial x^2} - \frac{1}{C_0^2} \frac{\partial^2 \psi}{\partial t^2} = \frac{1}{i\omega\rho_0} \left\{ \frac{\partial q}{\partial t} - \frac{\partial f_{ei}}{\partial x} + \frac{\partial^2 T_{ij}}{\partial x_i \partial x_j} \right\} = -4\pi \, f(x,t) \, .$$

This inhomogeneous wave equation can be integrated by use of the Kirchoff method (Stratton (1941) and Jackson (1962)) to yield:

$$\psi(x,t) = \frac{\int dV \, [f]}{|x - x'|} + \frac{1}{4\pi} \int dS \, [1/R \, \partial\psi/\partial n - \partial/\partial n(1/R)\psi + 1/C_0 R \, \partial R/\partial n \, \partial\psi/\partial t] \, .$$

This solution, when applied to our specific problem with the properties of $\partial[\;]/\partial x_i$ and $\partial[\;]/\partial y_i$, as well as the divergence theorem, yields the desired results:

$$4\pi C_0^2(\rho - \rho_0) = 4\pi P = \int [\partial q/\partial t_i] \, dV/R - \partial/\partial x_i \int [f_{ei}] \, dV/R + \partial^2/\partial x_i \partial x_j \int [T_{ij}] \, dV/R -$$

$$- \int l_i \, [\partial \rho u_i/\partial t] \, dS + \partial/\partial x_i \int l_i \, [2\rho_0 U_i u_j + \rho_0 u_i u_j + P_{ij}] \, dS/R \, .$$

APPENDIX B: MIXTURE THEORY

A.B.Wood (1932) showed that the sonic speed could be calculated for an air-bubble/water mixture by use of the mixture density (ρm) and the mean compressibility (km). The mixture can be treated as a continuous medium when the bubble diameter (d) and spacing between the bubbles (D) are much less than the wavelength of sound. In the case of low frequencies, for the mixture with a volume fraction (X) of gas we can calculate the mean density and compressibility as follows:

$$\rho_m = (1 - x)\rho_l + x\rho_g$$

$$K_m = \frac{-dv_m}{v_m \, dP} = - \frac{dv_l}{v_l \, dP} \frac{v_l}{v_m} + \frac{dv_g}{v_g dP} \frac{v_g}{v_m} = (1 - x)K_l + x \, K_g \quad .$$

This imples that a state of equilibrium prevails and the mixture mass is conserved, and the pressure, P, is uniform throughout the mixture (a low frequency assumption). Since the sonic speed is

$$C^2 = dP/d\rho = (\rho K)^{-1},$$

we have

$$C_m^2 = C_{mix}^2 = [(1 - x)\rho_l + x\rho_g] \, [(1 - x)K_l + xK_g]$$

$$C_m^2 = (1 - x)/C_l^2 + x^2/C_g^2 + (x)(1 - x) \frac{\rho_g^2 C_g^2 + \rho_l^2 C_l^2}{\rho_l \rho_g C_l^2 C_g^2} \quad .$$

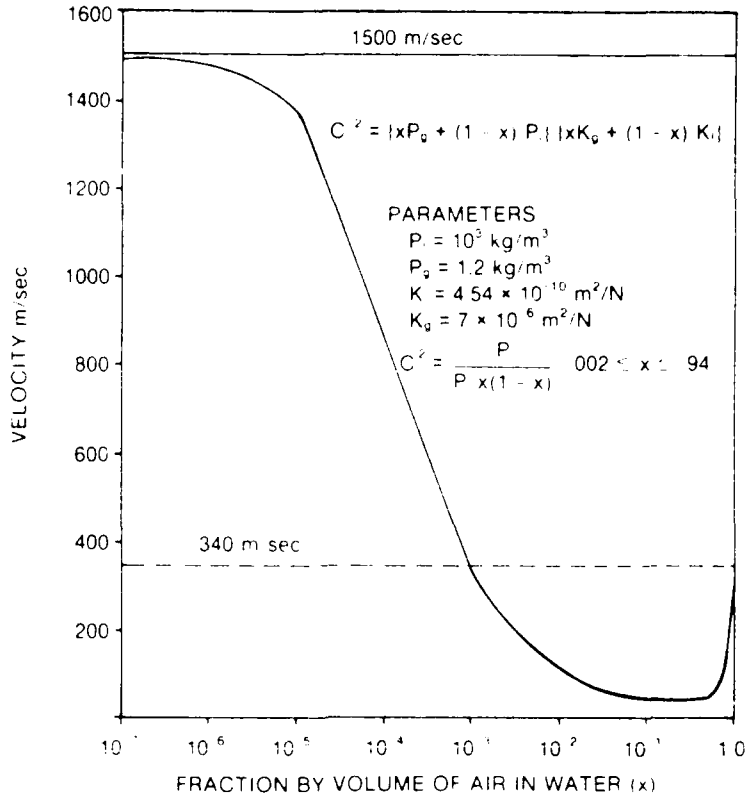

Figure B-1. Low Frequency Approximation for the Mixture Speed

The expression for the sonic speed poses the question of whether the gas compressibility is described by an isothermal or adiabatic process, especially since the single phase sonic speed is known to be adiabatic. However, in the case of an air-bubble/water mixture, the controlling physical factor is the transfer of the heat generated in bubble compression to the surrounding liquid. If the transfer is rapid, then the bubble oscillation is isothermal, $(\partial v/\partial P = -v/P,\ K_g = 1/P)$, as compared to the adiabatic condition $(\partial v/\partial P = -v/\gamma P,\ K_g = 1/\gamma P)$. Thus, in use of the above equations one must use either for the adiabatic or isothermal case, $C_{gi} = C_{ga}/\sqrt{\gamma}$. Isothermal conditions are most likely to prevail for air-bubble/water mixtures due to the large thermal capacity of water. Examination of the above expressions shows that as $x \to 0$, $C_m^{-2} \to C_l^{-2}$, and as $x \to 1$, $C_m^{-2} \to C_g^{-2}$, as one would expect. The striking characteristic revealed by these equations (shown in figure B-1) is the sharp reduction in the sonic velocity at small volume fractions; i.e., X=0.002 → Cm=225 m/sec. These equations may be approximated for the air/water mixture:

$$C_m^2 = \frac{\gamma P}{\rho_l x\,(1 - x)} \xrightarrow{\gamma = 1} \frac{P}{\rho_l x\,(1 - x)}$$

$$C_m\ (x = 0.5) = 20 \text{ m/sec}$$

Karplus (1958) used an acoustic tube to determine the standing wave pattern as a function of air volume fraction. His results are shown in figure B-2. Close agreement was found between the inferred sonic speeds

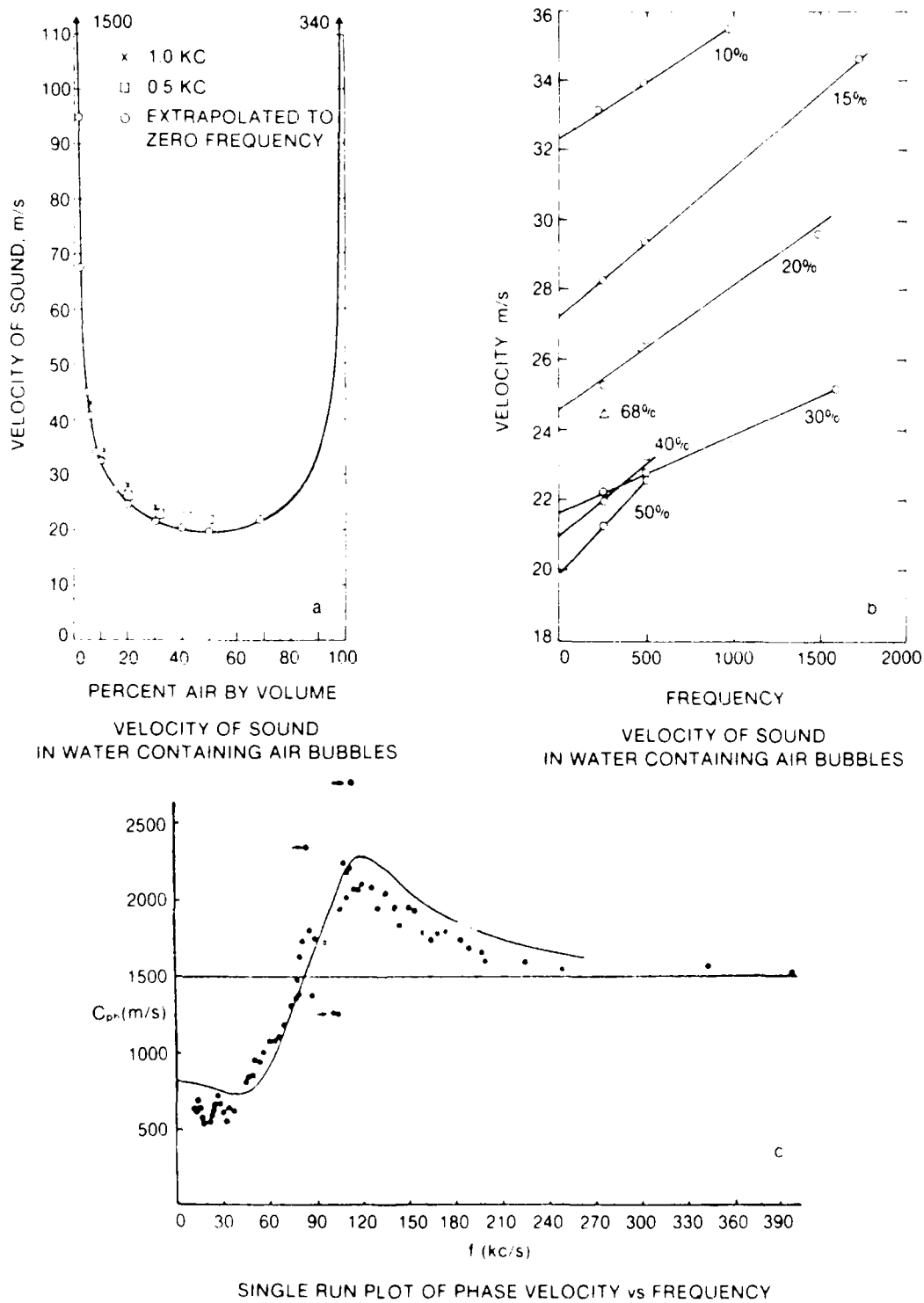

Figure B-2. Measured and Computed Mixture Sonic Speeds. a) Measured Mixture Speed vs. Volume Fraction at 500 and 1000 Hz, Karplus (1958); b) Measured Dispersive Character of Mixture Speed Below 2000 Hz, Karplus (1958); c) Measured and Computed Mixture Sonic Speed Showing the Behavior Below, At, and Above Resonance, Fox, et al. (1955)

and results calculated with Wood's expressions. Similar results have also been observed at the low frequencies by Campbell and Pitcher (1955). These results are also observed at the higher frequencies above and below resonance. Several studies and texts have been written on this subject and are listed in the references. An example of the agreement between theory and measurement near the vicinity of bubble resonance is shown in figure B-2c. It is important to note that most calculations performed at these higher frequencies use $Km = K_1 + Kg$, rather than the Wood approach $Km = (1 - x)K_1 + xKg$. This difference is unimportant near resonance and for small volume fraction but is important as one approaches the low frequencies of interest to this paper. One can show that the correct expression is:

$$\frac{1}{C^2} = \frac{(1 - x)^2}{C^2} + \frac{1}{C_m^2((1 - \omega^2/\omega_0^2) + 2i\delta\,\omega/\omega_0)},$$

when h.f. and l.f. are the high frequency and low frequency values of the sonic speed.

REFERENCES

Bachmann, W., and R.B. Williams, 1975: 'Oceanic Acoustic Modeling: Proceedings of a Conference Held at SACLANTCEN on 8-11 Sept. 1975.' SACLANTCEN Conf. Proc. 17(2) -- Bubbles NATO SACLANT ASW RES. CENTRE, LaSpezia, Italy

Bannister, R.W., 1986: 'Deep Sound Channel Noise from High-Latitude Winds,' Journal of the Acoustical Society of America 79(1), 41-48

Brekhovskikh, L.M., 1967: 'Generation of Sound Waves in a Liquid by Surface Waves,' Soviet Physics, Acoustics 12(3), 323-350

Browning, D.G., et al., 1981: 'Vertical Directionality of Low Frequency Ambient Noise in the South Fiji Basin,' Journal of the Acoustical Society of America 70(S1), S66a (also NUSC TD 6611, Jan. 1982)

Browning, D.G., et al., 1982: 'Shallow Water Ambient Noise: Offshore Measurements at 20-10,000 Hz.' NUSC TD 6825, NUSC, New London, CT

Burgess, A.S., and D.J. Kewley, 1983: 'Wind-Generated Surface Noise Source Levels in Deep Water East of Australia,' Journal of the Acoustical Society of America 73(1), 201-210

Carey, W.M., and R.A. Wagstaff, 1986: 'Low-Frequency Noise Fields,' Journal of the Acoustical Society of America 80(5), 1523-1526

Carey, W.M., and R.A. Wagstaff, 1985: 'Low-Frequency Noise Fields and Signal Characteristics,' Ocean Seismo-Acoustics: Low-Frequency Underwater Acoustics, T. Aka and J.M. Berkson, eds., Plenum Press, 753-766

Carey, W.M., and M.P. Bradley, 1985: 'Low-Frequency Ocean Surface Noise Sources,' Journal of the Acoustical Society of America, 78(S1)

Cato, D.H., 1976: 'Ambient Sea Noise in Waters Near Australia,' Journal of the Acoustical Society of America 60(2), 320-328

Dowling, A.P., J.E. Ffowcs Williams, 1983: Sound and Sources of Sound, John Wiley & Sons, NY

Ffowcs Williams, J.E., 1969: 'Hydrodynamic Noise.' Annual Review of Fluid Mechanics, W.R. Sears and M. Van Dyke, eds. Annual Reviews, Inc. Palo Alto, CA, 197-222

Fitzgerald, J.W., and R.H. Mellen, 1982: NUSC cont. N00140-82-M-ST20

Fitzpatrick, H.M., and M. Strasberg, 1959: 'Hydrodynamic Sources of Sound.' DTMB Rept 1269, NSRDC, Carderock, MD

Fox, F.E., et al., 1955: 'Ambient-Noise Directivity Measurements.' Journal of the Acoustical Society of America 27(3), 534-539

Furduev, A.V., 1966: 'Undersurface Cavitation as a Source of Noise in the Ocean,' Atmospheric and Oceanic Physics, 2(235), 314-320

Goncharov, V.V., 1970: 'Sound Generation in the Ocean by the Interaction of Surface Waves and Turbulence.' Izv., Atmospheric and Oceanic Physics 6(11), 1189-1196

Hinze, J.O., 1959: Turbulence, McGraw-Hill Book Co., NY

Hughes, B., 1976: 'Estimates of Underwater Sound (and Infrasound) Produced by Nonlinearly Interacting Ocean Waves,' Journal of the Acoustical Society of America 60(5), 1032-1039

Huon-Li, 1981: 'On Wind-Induced Underwater Ambient Noise.' NORDA TN 89, NORDA, NSTL, MS

Jackson, J.D., 1962: Classical Electrodynamics, John Wiley & Sons, NY

Kerman, B.R., 1984: 'Underwater Sound Generation by Breaking Waves.' Journal of the Acoustical Society of America 75(1), 149-165

Karplus, H.B., 1958: 'The Velocity of Sound in a Liquid Containing Gas Bubbles,' Armour Research Foundation, University of Illinois, Proj. c00-248, TID-4500

Kibblewhite, A.C., and K.C. Ewans, 1985: 'Wave-Wave Interactions, Microseisms, and Infrasonic Ambient Noise in the Ocean,' Journal of the Acoustical Society of America 78(3), 981-994

Knudsen, V.O., R.S. Alford and J.W. Emling, 1948: 'Underwater Ambient Noise,' Journal of Marine Research 7, 410-429

Kuo, E.Y.T., 1968: 'Deep-Sea Noise Due to Surface Motion,' Journal of the Acoustical Society of America 43(5), 1017-1024

Latham, G..V., and A.A. Nowroozi, 1968: 'Waves, Weather and Ocean Bottom Microseisms,' Journal of Geophysical Research 73(12), 3945-3956

Lighthill J., 1979: Waves In Fluids, Cambridge University Press, Cambridge, UK

Lloyd, S.P., 1981: 'Underwater Sound from Surface Waves According to the Lighthill-Ribner Theory,' Journal of the Acoustical Society of America 69(2), 425-435

Martin, R.L., 1985: 'Effects of the Ocean Boundaries and Bottom Topography on Acoustic Ambient Noise Fields in the Ocean,' NORDA TN 323, NORDA, NSTL, Mississippi

McDaniel, S.T., 1987: 'Subsurface Bubble Densities from Acoustic Backscatter Data,' ARL/TM-87-57, Applied Research Lab, Penn. State Univ., State College, PA 16804

Mellen, R.H., 1987: private communication.

Minnaert, M., 1933: 'Musical Air-Bubbles and Sounds of Running Water.' Philosophical Magazine 10, 235

Nichols, R.H., 1981: 'Infrasonic Ambient Noise Measurements: Eleuthera,' Journal of the Acoustical Society of America 69(4), 974-981

Ross, D., 1976: Mechanics of Underwater Sound, Pergamon Press, NY

Shang, E.C., and V.C. Anderson, 1986: 'Surface-Generated Noise Under Low Wind Speed at Kilohertz Frequencies,' Journal of the Acoustical Society of America 79(4), 964-971

Strasberg, M., 1984: 'Hydrodynamic Flow Noise in Hydrophones,' Adaptive Methods in Underwater Acoustics, H. Urban (ed.), Reidel, 125-141

Stratton, J.A., 1941: Electromagnetic Theory, McGraw-Hill Book Co., NY

Su, M.Y., A.W. Green and M.T. Bergin, 1984: 'Experimental Studies of Surface Wave Breaking and Air Entrainment,' Gas Transference at Water Surfaces, W. Brutsaert and G. Jirka (eds.), Reidel Press, pp 211-219

Thorpe, S.A., 1986: 'Measurements with an Automatically Recording Inverted Echo Sounder: Aries and Bubble Clouds,' Journal of Physical Oceanography 16, 1462-1478

Thorpe, S.A., 1986: 'Bubble Clouds: A Review of Their Detection by Sonar, of Related Models, and of How Kv May be Determined.' Oceanic Whitecaps and Their Role in Air-Sea Exchange Processes, Reidel in assoc. with Galway Univ. Press, 57-68

Thorpe, S.A., 1982: 'On the Clouds of Bubbles Formed by Breaking Wind-Waves in Deep Water, and Their Role in Air-Sea Gas Transfer.' Philosophical Transactions of the Royal Society of London, A304, 155-210

Urick, R.J., 1984: Ambient Noise in the Sea. U.S.G.P.O.: 1984 - 456-963, Washington, D.C.

Von Winkle, W.A., and D.G. Browning, 1985: 'Vertical Noise Directionality in the Deep Ocean: A Review,' Journal of the Acoustical Society of America 78(S1) (also NUSC TD 7561)

Wagstaff, R.A., 1981: 'Low-Frequency Ambient Noise in the Deep Sound Channel--The Missing Component,' Journal of the Acoustical Society of America 69(4), 1009-1014

Wenz, G.M., 1962: 'Acoustic Ambient Noise in the Ocean: Spectra and Sources,' Journal of the Acoustical Society of America 34, 1936-1956

Wilson, J.H., 1983: 'Wind-Generated Noise Modeling,' Journal of the Acoustical Society of America 73(1), 211-216

Wittenborn, A.F., 1976: 'Ambient Noise and Associated Propagation Factors as a Function of Depth Wind Speed in the Deep Ocean,' Tracor Rept. T76RV5060, DTIC(AD 006902), Alexandria, VA

Wood, A.B., 1932/1955: A Textbook of Sound, G. Bell and Sons Ltd., London, 360-364

Worley, R.D., and R.A. Walker, 1982: 'Low-Frequency Ambient Ocean Noise and Sound Transmission over a Thinly Sedimented Rock Bottom,' Journal of the Acoustical Society of America 71(4), 863-870

Wu, Jin, 1981: 'Bubble Populations and Spectra in the Near-Surface Ocean: Summary and Review of Field Measurements,' Journal of Geophysical Research 86 (C1), 457-463

Yen, Nai-Chyuan and A.J. Perrone, 1979: 'Mechanisms and Modeling of Wind-Induced Low-Frequency Ambient Sea Noise,' NUSC TR 5833, Feb. 1979

INITIAL DISTRIBUTION LIST

Addressee	No. of Copies
CNA	3
DTIC	2
DARPA/TACTICAL TECHNOLOGY OFFICE (C. Stuart)	1
CNO (OP-952; NOP-096)	2
CNR (OCNR-00, -10; -11; -1125 Marshall Orr, L. Johnson, R. Robracta, A. Brandt; -13 K. Dial, M. Briscoe; E. Chaika; ONT-23)	11
NAVAIRSYSCOM (NAIR-93; -933)	2
SPACE & NAV WARFARE SYS CMD (PMW-180 J. P. Feuillet, J. Synsky, CAPT K. Evans, CAPT R. Witter)	4
NAVSEASYSCOM (SEA-63)	1
NRL (NRL 5100 D. Bradley; 5120 O. Diachock (3 cys); 5160, F. Erskine, W. Kuperman, B. E. McDonald; 5130 N. Yen,	8
NOARL (TD W. Moseley, 200 R. Wagstaff, E. Franchi; 240 R. Farwell, H. Assanai)	5
NADC	1
NCSC (D. Fields)	1
NOSC (541B H. Bucker(3 cys); 732 D'Amico; 7304 N. Booth)	5
DTRC CADEROCK LAB (M. Strassberg; M. Sevick (3 cys))	4
NSWC WHITE OAK LAB (Code R-43 G. Gaunaurd)	2
NPS (Dr. H. Medwin, Dr. J. Nystuen)	2
NUSC DET WEST PALM BEACH (R. Kennedy)	3
APL/JOHNS HOPKINS (G. Smith (3 cys))	3
JOHNS HOPKINS UNIVERSITY (A. Prosperetti (3 cys), E. Fitzgerald)	4
APL/U. WASHINGTON (R. Spindel (2 cys), T. Ewart, E. Thoros)	4
ARL/PENN STATE (S. McDanniels (2 cys), D. McGammon)	3
ARL/U. TEXAS (K. Focke, J. Shooter, P. Vidmar, E. Westwood, S. Mitchell, N. Bedford)	6
MPL/SCRIPPS (F. Fisher, W. Hodgkiss, M. Buckingham, D. Jacobs, S. Webb)	5
WOODS HOLE OCEAN. INSTI. (S. Rajan, G. Frisk, J. Lynch, J. Doutt)	4
U. OF MIAMI (F. Tappert, H. DeFarrari, T. Yamamotto)	3
U. OF MISS. (L. A. Crum, R. A. Roy, S. W. Yoon, A. R. Kolaini, M. Nicholas)	5
BOLT BERANEK & NEWMAN, INC. (P. Cable, S. Marshall, W. Marshall),	3
SAI CORP., McLean, VA (A. Eller, R. Cavanaugh, C. Spofford)	3
SAI CORP., New London, CT (F. DiNapoli, R. Evans, W. VonWinkle)	3
PSI, McLean, VA (R. Brunson)	2
PSI, Sledell, LA (M. Bradley)	2
PSI, New London, CT (J. Davis)	2
TRW (S. Gerben)	1
MIT (I. Dyer, K. Melville, A. Baggeraer, H. Smedt)	4
U. CONN., AVERY POINT (E. Monahan, Dr. R. Mellen)	2
GEORGIA TECH. (P. Rogers)	2
CATHOLIC UNIVERSITY (J. McCoy, M. Beran, R. Urick)	3
BBN, Arlington, VA (H. Cox, J. Nitsche)	2
BBN, New London, CT (P. Cable, W. Marshall, J. Hanrahan)	3
BBN, Cambridge, MA (J. Barger, R. Collier, J. Heines)	3

INITIAL DISTRIBUTION LIST (CONT'D)

Addressee	No. of Copies
DEFENCE SCIENTIFIC ESTABLISHMENT (Dr. Richard Bannister)	1
DEFENCE RES. EST. PACIFIC (Dr. R. Chapman)	1
DEFENCE RES. EST. ATLANTIC (Dr. Harold Merklinger)	1
R.A.N. RESEARCH LAB. (Dr. Douglas Cato)	1
ADMIRALTY RES. EST. (Dr. G. C. Jackson, G. J. Kirby (2), Dr. David Weston, Dr. R. Marrett)	5
Atlantic Applied Research Corp. Dr. P. J. Stein 4 A Street Burlington, MA 01803	1
Atmospheric Envirnoment Service Dr. B. Kerman Canada Centre for Inland Waters PO Box 5050, Burlington Ontario Canada	3
British Aerospace P. F. Dobbins, FPC 400 PO Box 5 Filton Bristol BS12 7AW, UK	1
Centre for Studies of Nonlinear Dynamics, La Jolla Institute, Dr. M. Longuet-Higgins PO Box 1434, La Jolla, CA 92038	1
Defense Science & Technology Organization Dr. D. H. Cato Maritime System Division PO Box 706, Carlinghurst NSW 2010, Australia	1
Industrial Acoustics Laboratory Dr. L. Bjorno Technical University of Denmark Lyngby,DK-2800, Denmark	3
Institute of Ocean Sciences Dr. D. Farmer, Mr. Y. Xie PO Box 6000, Sidney, British Columbia V8L 4B2, Canada	2
Jasco Research Ltd. Mr. M. Greening 9865 W. Saanich Rd., Sidney, British Columbia V8L 3S1 Canada	2

INITIAL DISTRIBUTION LIST (CONT'D)

Addressee	No. of Copies
Marconi Maritime, Applied Research, Dr. D. Burton, Dr. W. Fitzgerald Cambridge Science Park, Unit 33 Milton Road, Cambridge CB4 4 FX, UK	2
Marconi Underwater Systems Ltd. P. A. Crowther, H. Griffiths, A. Hansla Croxley Mill, Watford Herts WD2 8YR. UK	3
Nansen Remote Sensing Center Ms. H. Sagan Edv Griegsv 3A N-5037 Solheinsvik, Norway	1
Neptune Technologies Inc. Dr. J. H. Wilson P.O. Box 1235 San Clementa, CA 92672	1
Office of Naval Research Dr. D. Feit, L. Jendro European Centre, 223 Old Marylebone Road, London, NW1 5TH, UK	2
Proudman Oceanographic Laboratory Dr. P. D. Thorne Bidston Observatory Birkenhead, Merseyside L43 7RA UK	1
Rensselaer Polytechnic Inst. Dr. W. Siegmann Dept. of Math. Sciences Troy, NY 12180	5
Science Applications Dr. W. Denner 205 Montecito Avenue, Monterey CA 93940	1
Tohoku University Dr. N. Ebuchi Department of Geophysics, Faculty of Science Aoba, Sendai 980, Japan	1
Topexpress Ltd. Dr. J. F. Scott Poseidon House, Castle Park Cambridge CB3 ORD UK	1

INITIAL DISTRIBUTION LIST (CONT'D)

Addressee	No. of Copies
University of Auckland Dr. A. Kibblewhite (2), Dr. Gary Bold Dept. of Physics Auckland, New Zealand	3
University of Cambridge Dr. J. E. Ffowcs Williams Dr. H. Pumfrey Dept. of Engineering Cambridge CB2 1PZ UK	2
University of Cambridge Mr. K. Lunde Dept. of Appl. Math. & Theor. Physics Cambridge CB3 9EW UK	1
University of Southampton Dr. S. A. Thorpe Department of Oceanography Southampton SO9 5NH UK	1
Yard Ltd. Dr. G. J. M. Copeland Yard Ltd., Charing Cross Tower, Charing Cross Glasgow G2 4 PP, U.K.	1
Dr. A. Purcell Box 1388 Lunenburg, Nova Scotia BOJ 2CO Canada	1